Geological Society of America Bulletin

Tightening the Belt: Paleomagnetic-stratigraphic constraints on deposition, correlation, and deformation of the Middle Proterozoic (ca. 1.4 Ga) Belt-Purcell Supergroup, United States and Canada

D.P. Elston, R.J. Enkin, J. Baker and D.K. Kisilevsky

Geological Society of America Bulletin 2002;114;619-638
doi: 10.1130/0016-7606(2002)114<0619:TTBPSC>2.0.CO;2

Tightening the Belt: Paleomagnetic-stratigraphic constraints on deposition, correlation, and deformation of the Middle Proterozoic (ca. 1.4 Ga) Belt-Purcell Supergroup, United States and Canada

D.P. Elston
6300 Country Club Drive, Flagstaff, Arizona 86004, USA

R.J. Enkin*
J. Baker
Geological Survey of Canada–Pacific, Sidney, British Columbia V8L 4B2, Canada

D.K. Kisilevsky
Petrel Robertson Consulting, Ltd., Calgary, Alberta T2P 3C4, Canada

ABSTRACT

The Belt-Purcell Supergroup crops out in Montana, Idaho, Washington, British Columbia, and Alberta. It is the largest and most intensively studied Middle Proterozoic succession in North America. A major paleomagnetic survey of the Belt-Purcell basin in Montana was carried out by the U.S. Geological Survey between 1975 and 1985, but only partial results have been published. We reanalyze these data and add new data from the Canadian part of the basin. Results come from >2700 samples (mostly red beds) from 93 localities, spanning 13 formations or members of formations. They typically exhibit stable magnetizations carried by hematite in detrital specularite grains and pigment. Coherent paleomagnetic directions have either southwest declinations and moderate positive inclinations (normal polarity) or northeast declinations and moderate negative inclinations (reverse polarity). These directions clearly pass fold and reversal tests. A stratigraphically coherent directional swing and a reproducible polarity zonation indicate that the stable magnetization is primary and was acquired during the course of deposition. U-Pb dates suggest an ~50 m.y. duration of deposition of the upper part of the Belt-Purcell Supergroup. The limited amount of apparent polar wander and the few polarity reversals recorded in the Belt-Purcell deposits are similar to the rate of polar wander and a long interval of stable polarity observed for the middle Cretaceous. An apparent incompatibility between early Middle Proterozoic (Elsonian) paleomagnetic poles from different regions of North America is now resolved; the Belt-Purcell poles are middle Elsonian in age and form the southern extreme point on a hairpin loop of the 1500–1400 Ma part of a refined Elsonian apparent polar wander path.

Keywords: Apparent polar wander, Belt-Purcell Supergroup, Middle Proterozoic, North American Cordillera, paleomagnetism, red beds.

INTRODUCTION

The Belt-Purcell Supergroup is the largest, most intensively studied Middle Proterozoic stratigraphic succession in western North America. It crops out in Montana, Idaho, Washington, British Columbia, and Alberta (Fig. 1). The Belt-Purcell section attains a thickness of as much as 20 km (Harrison, 1972; McMechan, 1981). At places, the strata host rich deposits of lead, zinc, copper, and silver, including the world-class Sullivan sedimentary-exhalative Zn-Pb orebody of southeast British Columbia. Despite more than a century of study and mapping beginning with Walcott (1899), major questions have remained concerning the basin's tectonic setting and the time and duration of deposition. Origins for the Belt-Purcell basin proposed by various researchers (reviewed by Link et al., 1993) include an intracratonic rift basin, a marine-trailing continental margin, an episutural basin, and a meteorite-impact basin.

Paleomagnetic data can be applied in a number of ways that could elucidate questions on the age and origin of the Belt-Purcell basin. Paleomagnetic directions and polarities can serve to correlate stratigraphic packages, identify sedimentary-facies changes, and establish the age and duration of deposition. Moreover, when paleomagnetic poles from the Belt-Purcell basin are compared to poles from other parts of Laurentia (i.e., Precambrian North America), a refined reconstruction of the Middle Proterozoic paleogeographic setting becomes possible. On a local scale, diverging declinations for horizons sampled at different localities are the signature of vertical-axis rotations, caused by Cretaceous and Cenozoic compressional deformation and Cenozoic extension, which can be recognized and corrected. Finally, diagenetic events arising from deep burial and externally imposed thermal events can be identified, thereby characterizing the nature and extent of remagnetizations.

Paleomagnetic techniques have been applied to Belt-Purcell studies from the early years of the discipline. Collinson and Runcorn

*Corresponding author; e-mail: enkin@pgc.nrcan.gc.ca.

GSA Bulletin; May 2002; v. 114; no. 5; p. 619–638; 9 figures; 4 tables.

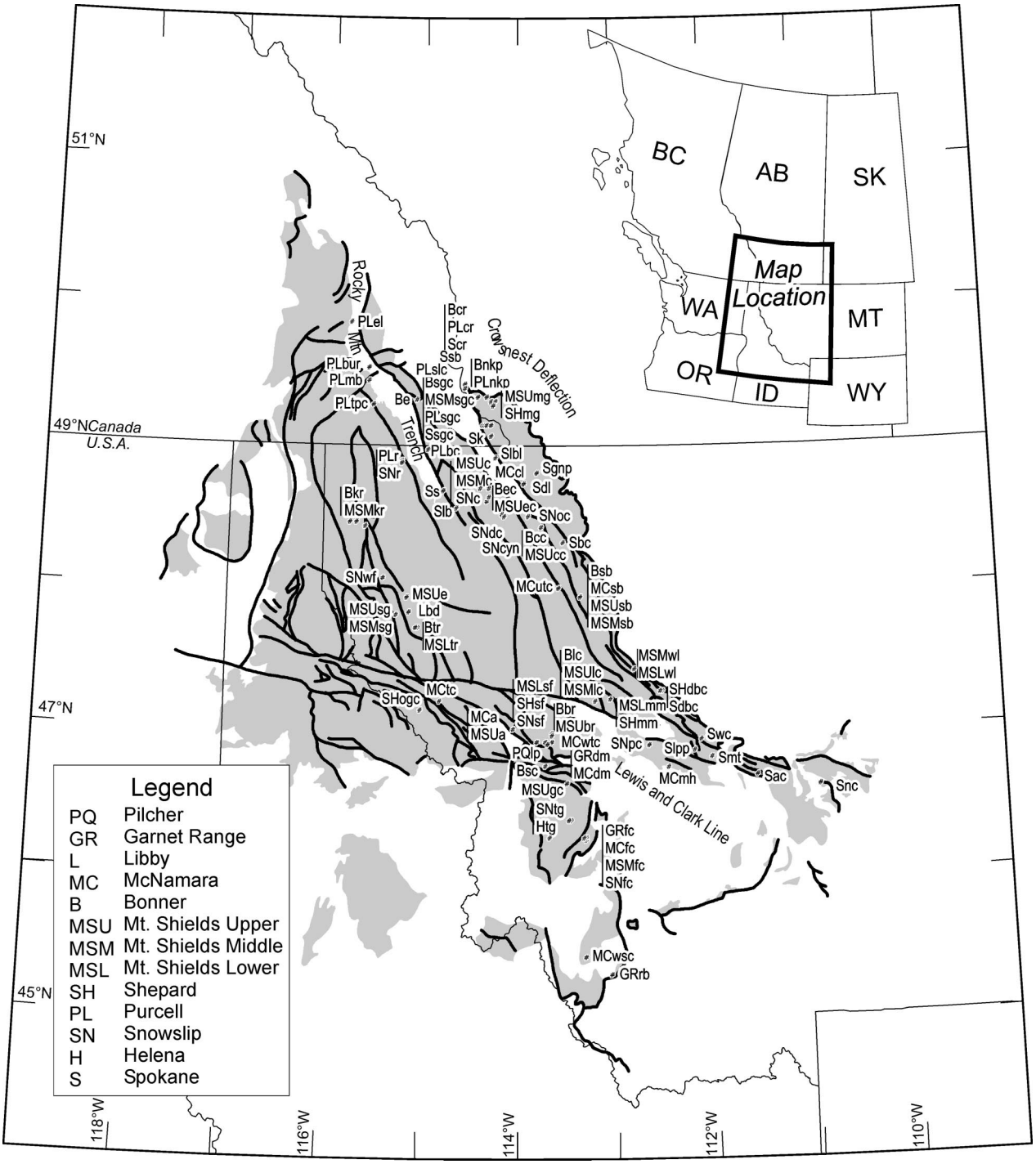

Figure 1. Sampling locations in the Belt-Purcell basin. Points mark localities consisting of 3–220 samples (median of 28 samples) usually spread over several sites or a long magnetostratigraphic section. The formations sampled are identified by capital letters and the locations by small letters (e.g., Snc stands for Spokane Formation at Newlan Creek; see Table 1 for locality names). Localities with more than one sampled formation are indicated by thin vertical bars. The Belt-Purcell outcrop is shaded gray, and the dark lines are faults (mostly Laramide thrust faults). Geology digitized from Winston (1986).

(1960) and Runcorn (1964) were interested primarily in the paleogeography of North America and Europe and the nature of the Proterozoic geomagnetic field. Norris and Black (1961) used paleomagnetism to reject the hypothesis that the curved thrust trace of the Lewis fault was caused by oroclinal bending. Black (1963) attempted to date the basin by paleomagnetic correlation with other North American poles. Although these studies fall short of current standards of laboratory analysis, the polarities and directions (noted in Ta-

ble 1) are remarkably consistent with those we report here, affirming the generally high stability of magnetization contained in these rocks.

Extensive paleomagnetic sampling of the Belt-Purcell basin deposits in Montana by the U.S. Geological Survey (USGS) took place between 1974 and 1984. A preliminary polar path and polarity zonation were reported by Elston and Bressler (1980) and were followed by an improved polar path and summary (Elston, 1984). This Belt-Purcell apparent polar wander path (APWP) subsequently was incorporated in a framework of interrelated stratigraphic and paleomagnetic correlations proposed for western North America (Link et al., 1993). The Canadian part of the basin was sampled by the Geological Survey of Canada (GSC) in 1995 and 1996 (Kisilevsky, 1998). Much of the USGS data and all of the GSC data are published here for the first time. We also have incorporated results of the small focused studies of Evans et al. (1975), Vitorello and Van der Voo (1977), and Morris and McMechan (1983).

GEOLOGY AND RADIOMETRIC AGES

Because of discontinuous exposures, sedimentary-facies changes, and an uneven mapping history, an array of poorly correlated formation names came into the literature. A coherent stratigraphy and framework for correlation, along with an understanding of the nature of the basin, was developed in the 1960s and 1970s as a consequence of a program of regional geologic mapping at 1:250 000 scale (Harrison, 1972). Results of regional stratigraphic studies are reported in the review by Link et al. (1993). We relate all formations to the stratigraphy in the Missoula and Glacier Park areas in the eastern basin (Table 2). The Belt-Purcell basin fill is strongly asymmetric; it consists predominantly of mudstone and siltstone in the eastern and central parts of the basin (where most of our sampling was done) and coarser sandstone in the west and locally in the south. Harrison (1972) divided the Belt-Purcell succession into four groups and noted that the sedimentary fill apparently accumulated without appreciable break. The Lower Belt Group was reported to consist of ≤10 km of deep-water turbidites of the Prichard Formation and its equivalents, at places penecontemporaneously intruded by ≤2 km of Moyie sills.

Shallow-marine conditions prevailed during deposition of all higher Belt-Purcell strata. The overlying Ravalli Group consists of the intensely red Spokane Formation and the dominantly green and subordinately red strata of the Empire Formation. Overlying these rocks is the gray Middle Belt Carbonate, which in the Missoula area and to the east consists solely of the Helena Formation. To the west, the Helena loses its distinct lithologic character and passes into dark siltites and subordinate carbonates of the Wallace Formation.

The uppermost ~5 km of the succession constitutes the Missoula Group. Red beds of the Missoula were a major focus of this study. Interbedded green and subordinately red argillite characterizes the Snowslip Formation, the basal unit of the Missoula Group. Interbeds of Purcell Lava, very near the top of the Snowslip, are found in the northern part of the basin. At the top of the Snowslip, a sharp, clean unconformity marks its contact with the overlying Shepard Formation (Whipple and Johnson, 1988; Höy 1993). It represents the only apparent break in sedimentation in the Missoula Group noted during geologic mapping and paleomagnetic studies. Siltite of the Shepard is characteristically dark, and red beds are rare and limited stratigraphically. The coarser-grained Mount Shields Formation overlies the Shepard. This conspicuously red formation is divided into lower, middle, and upper members. The middle and upper members contain interbeds of fine to coarse-grained sandstone. Red to purple, coarse-grained mica-bearing Bonner Quartzite overlies the Mount Shields Formation, the contact between these formations being gradational. The Bonner, in turn, grades upward into the argillitic, dark red and dark gray McNamara Formation. The coarser-grained Garnet Range Formation overlies the dark McNamara. Because the Garnet Range Formation and its equivalent, the upper member of the Libby Formation (Table 2), mark a transition to higher-energy, deeper-water conditions (Kidder, 1988), it may be that these rocks postdate the Belt-Purcell succession. Red beds appear near the base and near the top of the Garnet Range Formation, where it grades upward into the coarse-grained Pilcher Quartzite.

Other than syndepositional extensional tectonics, the Belt-Purcell basin was an island of stability in a larger region subjected to major rifting and orogenic events through the Middle and Late Proterozoic and Phanerozoic. Following a depositional hiatus of >700 m.y., Belt-Purcell strata were unconformably overlapped by the Middle Cambrian Flathead Sandstone. Although this interval of nondeposition is long enough to have seen the creation and destruction of two great oceans, little geologic activity seems to have affected the basin. Block faulting occurred during the Goat River orogeny at ca. 900–800 Ma (McMechan and Price, 1982), leading to rifting and deposition of the Late Proterozoic Windermere Group. Later, a section of Paleozoic carbonate and Mesozoic clastic strata was deposited, reaching 8 km in thickness in the vicinity of the Flathead fault in southeast British Columbia (Price, 1965). During the Late Cretaceous Laramide orogeny, strata of the Belt-Purcell basin were thrust against and over Paleozoic and Mesozoic strata. The west-to-east–directed thrusts had displacements ranging from a few kilometers near the Helena embayment to >100 km along the Lewis fault in southern Alberta (Price and Sears, 2001). Internally, the basin also has been cut by numerous thrust, strike-slip, and extensional faults of Cretaceous and Paleogene age.

Despite Proterozoic and Paleozoic burial and Mesozoic and Paleogene orogenesis, metamorphic grade recorded by the Belt-Purcell rocks is generally low. The grade increases with stratigraphic depth from east to west (Maxwell and Hower, 1967), locally in the west reaching as high as amphibolite facies at the bottom of the section. In the east, Missoula Group rocks are not obviously metamorphosed, but underlying rocks are metamorphosed to lower greenschist facies. In the west, strata above the middle Ravalli Group are metamorphosed to lower greenschist grade, and underlying strata to biotite grade (Harrison, 1972). During the Late Cretaceous Laramide orogeny in southern Canada, annealed fission tracks in apatite (Osadetz et al., 1995) indicate that temperatures exceeded 120 °C. However, fission tracks in zircon were not annealed, even in the lowest parts of the Lewis thrust sheet, indicating that temperatures probably did not exceed 230 °C anywhere in the sequence.

Several stratigraphic horizons and intrusive rock units have been dated radiometrically (Table 2). These dates, mostly published since the paleomagnetic work was done, provide a time context that previously was lacking. A maximum age for the Belt-Purcell section is provided by the Priest River Complex in northern Idaho. This basement to the Belt-Purcell has ca. 1576 Ma zircon ages (Evans and Fisher, 1986; Doughty et al., 1998). More definitively, the Moyie sills, which were intruded into still-wet sediments of the Prichard Formation (Höy, 1989), have concordant zircon ages between 1469 and 1457 Ma (Anderson and Davis, 1995; Sears et al., 1998). Stratigraphically higher, a bentonite layer in the Middle Belt Carbonate (Helena Formation) yielded a 1454 Ma zircon age (Aleinikoff et

TABLE 1. BELT-PURCELL SUPERGROUP LOCALITY MEANS

Locality	Code	Lat (°N)	Long (°W)	Strike (°)	Dip (°)	Step	*n*	D_g (°)	I_g (°)	D_s (°)	I_s (°)	*k*	α_{95} (°)	N/R	Comments
9. Pilcher Quartzite, Garnet Range Formation, and Libby Formation															
Lockwood Point and Wisherd Ridge	PQlp	46.92	113.80	86.7	5.5	590 °C	20	27.4	−41.3	25.2	−36.5	37.8	5.4	R	
Diamond Mountain	GRdm	46.90	113.68	119.0	25.0	550 °C	21	16.4	−63.2	21.8	−38.5	62.4	4.1	R	
Red Butte	GRrb	45.28	113.04			630 °C	14			36.4	−26.7	50.5	5.6	R	
Flint Creek	GRfc	46.25	113.33	223.0	40.0	630 °C	17	352.4	3.2	358.3	−27.0	63.2	4.5	R	X, rot.
Basin Draw	Lbd	47.77	114.10	158.2	21.1	590 °C	21	18.4	−42.9	29.0	−27.7	8.8	11.4	R	
8. McNamara Formation															
Diamond Mountain	MCdm	46.90	113.68	134.0	20.3	590 °C	12	19.7	−52.5	26.5	−33.5	34.3	7.5	R	
Flint Creek	MCfc	46.25	113.32	209.3	38.3	650 °C	23	10.1	−28.5	34.0	−33.6	12.6	8.9	R	
Alberton	MCa	47.01	114.05	124.2	18.3	550 °C	34	48.1	−51.3	44.6	−33.4	16.4	6.3	R	
Trout Creek	MCtc	47.20	114.80	70.0	9.0	550 °C	16	228.2	49.6	219.3	45.6	19.3	8.6	N	
							20	10.7	−38.4	7.7	−30.5	17.5	8.0	R	X, contam.
West Twin Creek	MCwtc	46.92	113.72	95.6	32.1	590 °C	56	33.5	−60.7	21.0	−30.6	10.1	6.3	N+R	
Upper Twin Creek	MCutc	48.00	113.58	339.0	26.5	550 °C	11	233.5	7.9	230.5	33.3	69.3	5.5	N	
Spotted Bear River	MCsb	47.93	113.35	335.8	43.5	590 °C	10	238.3	−0.1	235.5	42.9	35.5	8.2	N	
Cyclone Lake	MCcl	48.70	114.30	338.0	14.8	650 °C	7	19.9	−18.3	15.0	−27.7	38.7	9.8	R	
Meyers Hill	MCmh	46.73	112.45	11.0	19.0	590 °C	14	50.2	−26.5	40.3	−37.3	66.0	4.9	R	
Warm Springs Canyon	MCwsc	45.40	113.31	154.5	32.0	590 °C	12	32.3	−71.0	51.2	−41.0	27.3	8.5	N+R	
Blackfoot Canyon	MCbfc60	47.	114.			NRM	53			26.0	−43.0	30.0	4.0	R	X, (1)
7. Bonner Quartzite															
Spotted Bear River	Bsb	47.93	113.35	334.2	40.5	550 °C	27	228.4	−5.8	225.3	33.0	25.8	5.6	N	
Crystal Creek	Bcc	48.42	113.75	327.4	55.9	550 °C	31	222.5	−18.4	219.9	35.6	44.9	3.9	N	
Thompson River	Btr	47.71	115.06	184.0	25.0	550 °C	23	193.1	51.3	218.2	41.7	24.7	6.2	N	
Elelehum Creek	Bec	48.63	114.29	332.0	16.0	630 °C	29	219.1	31.7	213.5	46.2	38.5	4.4	N	
Lodgepole Creek	Blc	47.20	113.20	310.4	36.0	550 °C	5	213.6	7.6	211.1	43.3	85.9	8.3	N	
Schwartz Creek	Bsc	46.75	113.71	163.5	44.0	550 °C	16	312.1	68.0	275.7	32.1	16.9	9.2	N/R	X, rot.
Kootenai River 1	Bkr1	48.45	115.69	352.0	27.3	550 °C	36	220.8	11.7	213.0	31.2	79.6	2.7	N	
Kootenai River 2	Bkr2	48.42	115.61	10.2	51.0	550 °C	9	247.6	−3.7	237.3	37.8	63.4	6.5	N	
Blackfoot River	Bbr	46.92	113.64	109.0	25.0	550 °C	16	205.2	65.1	202.4	40.2	35.6	6.3	N	
Castle River	Bcr	49.27	114.26	130.5	10.6	PCA	11	231.2	51.4	229.3	41.0	59.9	5.9	N	
6. Mount Shields Formation, upper member															
North Kootenay Pass	Bnkp	49.39	114.57	177.7	27.7	PCA	4	190.2	51.2	215.9	38.8	60.7	11.9	N	
Sage Creek	Bsgc	49.14	114.28	14.1	5.7	PCA	14	222.6	33.5	219.1	36.1	45.9	5.9	N	
Elko	Be	49.31	115.08	167.7	22.6	PCA	10	218.6	53.0	230.5	33.9	63.7	6.1	N	
Castle River	Bcr61	49.3	114.2			16 mT	25			220.5	49.	14.	8.	N	X, (2) Kintla C
Spotted Bear River	MSUsb	47.93	113.35	334.9	41.9	550 °C	12	224.0	−3.7	219.1	35.1	42.5	6.7	N	
Crystal Creek	MSUcc	48.42	113.75	334.3	56.2	550 °C	114	42.4	24.5	41.7	−28.1	28.8	2.5	N+R	
Elelehum Creek	MSUec	48.60	114.31	325.6	18.7	590 °C	60	223.1	12.9	221.3	31.1	15.1	4.9	N+R	
Lodgepole Creek	MSUlc	47.20	113.20	313.8	37.9	550 °C	20	40.6	10.0	40.2	−27.8	51.1	4.6	N+R	
Coal Creek	MSUc	48.70	114.38	338.3	26.0	550 °C	70	46.1	−7.7	42.2	−31.5	23.3	3.6	R	
Elk Creek	MSUe	47.93	115.15	161.2	52.1	630 °C	25	339.7	−72.0	48.7	−36.2	32.3	5.2	N+R	
Snow Gulch	MSUsg	47.80	115.27	215.8	25.3	550 °C	80	32.6	−29.4	46.6	−27.7	30.3	2.9	R	
Alberton	MSUa	47.01	114.05	331.5	137.2	590 °C	94	283.5	58.5	39.5	−21.2	12.7	4.3	R+N	18 polarity changes
Blackfoot River	MSUbr	46.92	113.64	100.7	19.5	550 °C	213	31.3	−40.4	27.5	−21.9	23.3	2.0	R+N	16 polarity changes
Goose Creek	MSUgc	46.62	113.49	196.3	8.9	590 °C	20	57.4	−31.8	61.0	−25.7	25.6	6.6	R	
Mount Gladstone	MSUmg75	49.31	114.23	95.6	34.1	600 °C	6	240.8	65.0	211.7	38.0	69.5	8.1	R+N	(3) mean of sites
5. Mount Shields Formation, middle member															
Snow Gulch	MSMsg	47.80	115.27	215.8	25.3	550 °C	23	34.6	−15.3	41.4	−14.3	15.9	7.8	R	
Coal Creek	MSMc	48.70	114.38	335.0	27.0	550 °C	12	45.0	−2.7	42.3	−27.9	15.1	11.5	R	
Spotted Bear River	MSMsb	47.93	113.35	334.9	41.9	550 °C	5	39.1	12.4	36.8	−25.3	34.9	13.1	R	
Lodgepole Creek	MSMlc	47.20	113.20	313.8	37.9	550 °C	19	37.3	15.0	37.0	−22.7	20.4	7.6	R	
Flint Creek	MSMfc	46.24	113.29	224.7	44.3	590 °C	11	17.7	−16.4	37.1	−30.4	30.7	8.4	R	
Wood Lake	MSMwl	47.42	112.79	132.4	46.2	500 °C	7	356.0	−66.7	23.8	−26.0	20.4	13.7	R	
Kootenai River	MSMkr	48.45	115.77	318.0	25.0	550 °C	6	54.0	−4.3	54.9	−29.1	99.3	6.8	R	
Sage Creek	MSMsgc	49.14	114.33	38.1	18.0	PCA	5	55.1	−36.2	41.2	−39.4	48.8	11.1	R	
Windsor Mountain	MSMwm61	49.3	114.3			31 mT	4			18.	−12.5	24.	19.	R	X, (2) sill in Kintla B
4. Mount Shields Formation, lower member															
Sunflower Mountain	MSLsf	46.96	113.65	97.3	28.5	630 °C	89	21.0	−43.0	17.3	−15.3	18.4	3.6	R	
Thompson River	MSLtr	47.72	115.03	170.0	24.0	550 °C	22	19.0	−40.3	32.0	−26.1	47.6	4.5	R	
Wood Lake	MSLwl	47.42	112.79	132.0	53.7	500 °C	9	2.2	−71.8	29.6	−21.7	45.4	7.7	R	
Morrell Mountain	MSLmm	47.21	113.04	347.8	32.2	500 °C	21	31.4	0.4	26.8	−21.2	31.2	5.8	R	
Waterton Village	MSLwpv61	49.	114.			16 mT	13			46.	−34.	25.	8.5	R	X, (2) Kintla A
North Kootenay Pass	MSnkp63	49.4	114.6			16 mT	27			38.5	−39.5	23.	5.5	R	X, (4)
North Clark Range	MSncr63	49.3	114.3			16 mT	24			38.	−49.	24.	6.5	M	X, (4)
South Clark Range	MSscr63	49.0	114.1			16 mT	8			50.	−38.	40.	9.5	R	X, (4)
Essex	Mex64	48.	114.	331	57	NRM	39			38.	−27.	19.2	6.	R	X, (5) Missoula
3. Shepard Formation															
Sunflower Mountain	SHsf	46.96	113.65	109.0	15.0	590 °C	18	26.5	−36.1	25.5	−21.2	72.6	4.1	R	
Morrell Mountain	SHmm	47.21	113.04	350.5	35.6	500 °C	22	34.9	−2.9	27.6	−26.6	57.7	4.1	R	
Dearborn Canyon	SHdbc	47.27	112.53	130.5	17.6	550 °C	47	32.3	−42.4	33.8	−24.9	14.5	5.7	R	
Oregon Creek	SHogc	47.14	115.00	325.0	45.0	550 °C	23	33.4	24.9	34.5	−17.4	22.7	6.5	R	
Mount Gladstone	SHmg75	49.31	114.23	91.4	35.6	600 °C	8	51.1	−63.2	25.8	−33.8	29.4	10.4	R	(3) locality mean

TABLE 1. (*CONTINUED*.)

Locality	Code	Lat (°N)	Long (°W)	Strike (°)	Dip (°)	Step	*n*	D_g (°)	I_g (°)	D_s (°)	I_s (°)	*k*	α_{95} (°)	N/R	Comments
2P. Purcell Lava															
Blacktail Creek	PLbc	48.97	114.95	160.0	12.0	550 °C	7	223.6	58.5	229.9	47.5	26.1	12.0	N	X, contam.
							10	31.5	−30.7	35.0	−21.1	106.2	4.7	R	
Rexford	PLr	48.87	115.22	298.4	37.9	550 °C	10	206.1	20.2	204.3	58.0	9.3	16.8	N	X, contam.
							38	32.9	14.5	33.1	−23.3	57.1	3.1	R	
Castle River	PLcr	49.30	114.28	18.1	29.4	PCA	14	14.1	−70.8	22.0	−41.8	75.7	4.6	R	
Sage Creek	PLsgc	49.14	114.34	31.7	15.7	PCA	8	36.0	−27.0	28.0	−27.1	734.0	2.0	R	
							25	60.1	−40.4	44.0	−52.0	20.0	6.6	R	X, O
South Lost Creek	PLslc	49.43	114.57	147.7	41.8	PCA	6	352.5	−52.9	20.5	−25.2	48.3	9.7	R	
							13	176.7	−84.0	66.0	−58.0	39.1	6.7	R	X, O or partial O
North Kootenay Pass	PLnkp	49.39	114.56	166.5	28.9	PCA	15	17.9	−38.9	31.2	−20.8	46.7	5.7	R	
North Kootenay Pass '75	PLnkp75	49.40	114.56	167.0	30.0	600 °C	3	13.2	−39.5	28.5	−22.4	314.3	7.0	R	(3) locality mean
Bull River	PLbur	49.53	115.58	17.6	51.2	PCA	12	82.2	35.6	86.7	−11.6	68.8	5.3	R	X, rot.
Echo Lakes	PLel	49.85	115.79	354.7	71.1	PCA	37	42.8	12.6	28.8	−38.1	24.2	4.9	R	
Teepee Creek	PLtpc	49.28	115.53	2.3	42.5	PCA	8	244.9	34.8	205.3	65.9	103.9	5.5	N	X, O
							10	23.3	2.9	20.1	−11.9	34.5	8.3	R	
Mount Baker	PLmb	49.44	115.59	336.3	30.0	PCA	21	23.5	−2.6	18.4	−24.0	46.3	4.7	R	
Whistler Mountain	PLwhm61	49.3	114.3			16 mT	22			25.5	−17.5	4.	18.5	R	X, (2)
2. Snowslip Formation, Helena Dolomite															
Coal Creek	SNc	48.70	114.38	335.0	27.0	550 °C	38	32.7	5.2	31.1	−17.5	29.1	4.4	R	
Rexford	SNr	48.88	115.22	305.0	40.0	550 °C	19	31.1	29	31.5	−10.9	25.7	6.8	R	
Sunflower Mountain	SNsf	46.97	113.64	54.4	15.0	550 °C	7	34.8	−21.3	30.1	−15.7	78.2	6.9	R	
Ousel Creek	SNoc	48.49	113.88	138.8	27.3	550 °C	30	17.6	−50.8	27.4	−26.1	24.3	5.4	R	
Depuy Creek	SNdc	48.51	114.17	313.5	31.2	550 °C	43	28.3	2.1	26.3	−27.9	39.9	3.5	R	
Canyon Creek	SNcyn	48.49	114.14	329.2	51.4	550 °C	40	28.4	17.1	25.8	−27.3	35.3	3.9	R	
West Fisher Creek	SNwf	48.06	115.40	333.7	58.7	550 °C	21	30.7	31.1	33.9	−20.2	27.4	6.2	R	
Poorman Creek	SNpc	46.89	112.64	252.7	8.7	550 °C	26	213.5	19.8	216.3	25.1	39.2	4.6	N	Fm. bottom
Flint Creek (middle)	SNfcm	46.22	113.29	222.8	44.2	590 °C	44	26.9	−5.3	35.0	−14.8	14.4	5.9	R	
Flint Creek (lower)	SNfcl	46.22	113.29	222.4	47.0	550 °C	82	211.3	55.5	265.9	39.9	10.3	5.1	N	X, O, rot.
Trail Gulch	SNtg	46.36	113.46	318.0	20.0	550 °C	10	243.9	18.1	247.1	37.2	61.0	6.2	N	X, rot.
Pincher Ridge	SNpr61	49.3	114.1			16 mT	4			47.	−24.	34.	16.	R	(2)Siyeh Fm.
Donovan Creek	SNdvc60	47.	114.			NRM	23			234.	30.	20.	7.	N	(1)Miller Peak
Trail Gulch	Htg	46.36	113.47	318.0	25.0	550 °C	10	251.4	17.2	257.6	39.7	24.9	9.9	N	X, O, rot.
1. Spokane Formation															
Dearborn Canyon	Sdbc	47.27	112.51	131.0	20.0	550 °C	48	211.9	38.5	213.5	18.7	12.9	6.0	N	
Dutch Lakes site 1	Sdl1	48.72	113.94	316.0	16.0	550 °C	51	202	3.5	200.7	18.1	4.5	10.6	N	
Dutch Lakes site 2	Sdl2	48.72	113.94	118.0	14.0	550 °C	13	210	41.9	209.7	27.9	26.6	8.2	N	
Long Bow Lake	Slbl	48.91	114.22	80.0	2.0	590 °C	44	195	20.7	194.7	18.9	9.4	7.4	N	
Microwave Towers	Smt	46.80	112.00	252.0	23.0	630 °C	25	198.3	8.7	203.0	26.8	12.5	8.5	N	
Wolf Creek site 1	Swc1	46.93	112.12	159.5	17.4	590 °C	21	174.5	34.1	184.5	28.1	11.6	9.8	N	X, rot.
Wolf Creek sites 2 & 3	Swc2	46.93	112.12	243.9	8.2	590 °C	37	205.6	45.2	213.0	49.9	22.6	5.1	N	X, O
Bear Creek	Sbc	48.32	113.53	354.0	16.0	550 °C	27	218.1	35.3	207.4	45.4	16.4	7.1	N	X, O
Stryker	Ss	48.67	114.77	294.0	5.0	10 mT	12	239.2	43.7	242.3	47.7	30.4	8.0	N	X, O
Le Beau Creek	Slb	48.56	114.65	140.0	4.0	550 °C	14	205.7	44.3	207.2	40.6	63.0	5.0	N	X, O
Newlan Creek	Snc	46.60	110.90	128.0	30.0	550 °C	26	221.9	61.7	220.2	31.7	20.6	6.4	N	
Little Prickly Pear	Slpp	46.85	112.18	171.0	33.0	550 °C	17	212.9	72.9	243.3	44.0	20.3	8.1	N	X, O
Avalanche Creek	Sac	46.67	111.54	132.0	43.0	550 °C	136	255.2	58.5	239.6	19.0	13.4	3.4	N	X, O, rot.
Sage Creek	Ssgc	49.13	114.37	317.9	56.5	PCA	18	204.3	−29.7	205.7	23.0	32.1	6.2	N	
Castle River	Scr	49.33	114.32	120.8	35.4	PCA	18	147.0	88.3	208.2	53.8	16.8	8.7	N	X, O
Syncline Bk	Ssb	49.33	114.43	327.0	7.0	PCA	5	224.4	33.0	220.6	34.7	10.0	25.5	N	X, scatt.
Kishinena Creek	Sk	49.06	114.28	337.7	119.9	PCA	6	208.0	7.9	204.3	22.9	28.8	12.7	N	
Glacier National Park	Sgnp77	48.80	113.80	syncline		vect. sub.	14	199.9	39.5	201.7	40.2	61.0	5.1	N	X, (6) O, locality mean
Bad Rock Canyon	Sbrc64	48.	114.	293.	24.	NRM	9			240.	7.	11.8	16.	N	X, (5)
Prickly Pear Canyon	Sppc60	47.	112.			NRM	71			232.	55.	18.	4.	N	X, (1)
McDonald Creek	Smdc60	49.	114.			NRM	19			206.	39.	10.	8.	N	X, (1)
Glacier National Park	Sgnp60	49.	114.			NRM	44			225.	48.	15.	6.	N	X, (1)Grinnel
Pincher Ridge	Spr61	49.3	114.1			16 mT	16			212.5	50.5	52.	5.	N	X, (2)Grinnel
Prichard Formation															
Glacier National Park	PRgnp60	49.	114.			NRM	38			223.	29.	15.	6.	N	X, (1) Appekunny
West Castle River	PRwcr61	49.3	114.4			16 mT	17			202.	33.	25.	7.	N(R)	X, (2)Waterton

Note: Uppercase letters refer to the formation or member; lowercase letters identify the locality (see Fig. 1); lat and long give locality position; strike and dip give right-hand-rule bedding attitude. Step: demagnetization level used for most specimens, after determination from detailed demagnetization experiments (PCA—principal component analysis). Variables: *n*—number of specimens, *D*—declination, *I*—Inclination, *k*—Fisher precision, α_{95}—95% confidence interval about mean direction, subscript g—geographic coordinates, subscript s—stratigraphic coordinates, N/R—polarity. Comments: X marks localities rejected from the formation means given in Table 3. Previous work is noted in the comments column by numbers in parentheses: 1—Collinson and Runcorn (1960), 2—Black (1963), 3—Evans et al. (1975), 4—Norris and Black (1961), 5—Runcorn (1964), 6—Vitorello and Van der Voo (1977). The data from the 1960s are rejected because they used insufficient demagnetization. Others reasons for rejection are overprinting (O), contamination (contam.), vertical-axis rotation (rot.), and confidence interval > 15° (scatt.).

al., 1996; Evans et al., 2000). The Purcell Lava at the top of the Snowslip Formation is dated at 1443 Ma (Aleinikoff et al., 1996; Evans et al., 2000). Additionally, a sill in the Kitchener Formation, presumably a feeder for the Purcell Lava, has provided a zircon age of 1439 Ma (D.W. Davis *in* Brown and Woodfill, 1998).

Evans et al. (2000) have presented work on an ash layer near the base of the Libby Formation, toward the top of the Belt-Purcell succession at the town of Libby, Montana; the ash

TABLE 2. SCHEMATIC CORRELATION CHARF OF BELT-PURCELL FORMATIONS

This study		Coeur d'Alene	Clark Fork	Missoula	Glacier National Park 1984	Glacier National Park 1902	Cranbrook	Dating
Missoula Group	Pilcher Quartzite	Pilcher Quartzite		Pilcher Quartzite				
	Garnet Range Fm./Libby Fm.	Garnet Range Fm.	Libby Fm. upper mbr.	Garnet Range Fm.	Garnet Range Fm.			?*Whole-rock Rb/Sr: 930 Ma (Obradovich and Peterman, 1968)
	McNamara Fm. upper/ middle/ lower mbrs.	McNamara Fm.	Libby Fm. lower mbr.	McNamara Fm.	McNamara Fm.	Kintla Fm. mbr. D	Roosville Fm.	Libby basal tuff: 1401 ± 6 Ma (Evans et al., 2000)
	Bonner Quartzite	Bonner Quartzite	Bonner Quartzite	Bonner Quartzite	Bonner Quartzite	Kintla Fm. mbr. C	Phillips Fm.	
	Mount Shields Fm. upper, middle, and lower members	Striped Peak Fm.	Mount Shields Fm.	Mount Shields Fm.	Mount Shields Fm. 4, 3/2/1	Kintla Fm. mbr. B/A	Gateway Fm.	
	Shepard Fm.	Wallace Fm. upper mbr.	Wallace Fm. mbrs. 5, 4	Shepard Fm.	Shepard Fm.	Shepard Fm.	Sheppard Fm.	
	Purcell Lava		Wallace Fm. mbr. 3	Snowslip Fm.†	Purcell Lava	Purcell Lava	Nicol Creek Lava	Felsic flow at top: 1443 ± 7 Ma (Evans et al., 2000); sill in Kitchener: 1439.1 ± 2.4 Ma (Davis *in* Brown and Woodfill, 1998)
	Snowslip Fm.†				Snowslip Fm.†	Siyeh Fm.	Van Creek Fm.	
Middle Belt carbonate	Helena Fm.	Wallace Fm. Middle mbr.	Wallace Fm. mbr.	Helena Fm.	Helena Fm.		Kitchener Fm.	Helena bentonite: 1454 ± 9 Ma (Evans et al., 2000) >Intrusions in Yellowjacket Fm.: 1370 ± 2 Ma (Doughty and Chamberlain, 1996)
	Empire Fm.	Wallace Fm. lower mbr.	Wallace Fm. mbr. 1	Empire Fm.	Empire Fm.			
Ravalli Group	Spokane Fm.	St. Regis Fm.	St. Regis Fm.	Spokane Fm.	Grinnell Fm.	Grinnell Fm.	Creston Fm.	<Detrital zircons: 1590 Ma and older (Ross et al., 1992)
		Revett Fm.	Revett Fm.					
		Burke Fm.	Burke Fm.					
Lower Belt Group	Prichard Fm.	Prichard Fm. + Moyie sills	Prichard Fm. + Moyie sills	Greyson Fm./ Newland Fm.	Appekunny Fm.	Appekunny Fm.	Aldridge Fm. + Moyie sills	Moyie sills: ?1443 ± 10 Ma (Zartman et al., 1982); ?1445 ± 11 Ma (Höy, 1989); 1468 ± 2 Ma (Anderson and Davis, 1995); 1469 ± 2.5, 1457 ± 2 Ma (Sears et al., 1998); 1468 ± 2 Ma (Schandl and Davis, 2001) <Priest River Complex: 1576 ± 13 Ma (Evans and Fisher, 1986)
				Chamberlain Fm./Neihart Fm.	Altyn Fm.	Altyn Fm.	Fort Steele Fm.	

Note: Correlations are based on geochronological data tables in Harrison (1972), Winston (1986), Lind et al. (1993), and Höy (1993). Fm.—Formation
*"?" refers to questrionable age determinations, ">" marks minimum dates from units that crosscut Belt-Purcell strata, and "<" marks maximum dates from underlying basement or detrital zircons.
†Purcell Lava interbeds occur very near the top of the Snowslip. At the top of the Snowslip Formation, a sharp, clean dotted line marks its contact with the overlying Shepard Formation.

has provided a 1401 ± 6 Ma age (zircon). Belt-Purcell sedimentation is thought to predate intrusion of the Hellroaring Creek Stock near Kimberley, British Columbia, dated at 1365 ± 3 Ma (J.K. Mortensen, personal commun.). The foregoing ages contrast markedly with a much younger 930 Ma Rb/Sr whole-rock isochron from micaceous sedimentary rocks of the Garnet Range Formation and Pilcher Quartzite at the top of Belt-Purcell section (Obradovich and Peterman, 1968), which is now not accepted.

SAMPLING AND LABORATORY TECHNIQUES

Oriented samples were collected from localities across the Belt-Purcell basin (Fig. 1). Different sampling strategies were used in different places, depending on the nature of the outcrop and the problems being tackled. Often, one to several isolated sites of 5–15 samples were taken. At places, detailed magnetostratigraphic sampling was undertaken involving as many as 220 samples from a single section. For the purpose of assembling and reporting similar reliable data, we group as a "locality" all the sampling sites from stratigraphically similar positions in a single formation or member, separated by at most a few kilometers. Often, stratigraphic separations for individual cores (horizons) ranged from ~1 m to several meters. In most cases, the least weathered and least altered rocks were sampled. In some sections, samples were collected to investigate the nature and stability of magnetization in questionable horizons and were found wanting. They are noted as rejected samples at otherwise reliable sites. We were constantly testing the rocks for stability and reliability of magnetization as the geology of outcrops allowed.

The median number of specimens averaged together to obtain locality means is 26, equivalent to that from three or four standard paleomagnetic sites. Localities were almost always homoclines, and uniform to slightly varying bedding corrections were applied to all samples. Geographic positions and mean bedding attitudes are given in Table 1.

Nearly all localities were cored in the field by using a gasoline-powered drill; a very few were block sampled. Orientation was by magnetic compass, checked for consistency near and distant from the outcrop, and occasionally by sun compass. Measurements at the USGS Flagstaff Paleomagnetics Laboratory were made by using an SCT SQUID magnetometer. Earliest demagnetizations were done in a Helmholz-shielded oven, but later were done in a three-can Mu-metal–shielded oven having a residual field of <5γ. A standard Schonstedt alternating field (AF) tumbling demagnetizer was used mostly for demagnetization of magnetite-bearing rocks. At the GSC–Pacific laboratory, we used an Agico JR-5A spinner magnetometer, ASC TD48 furnace, and Schonstedt GSD-5 tumbling AF demagnetizer. Susceptibility was measured by using a Sapphire SI2B susceptibility meter to monitor for mineral changes during treatment.

The USGS measurements involved detailed pilot studies on ~10% of the samples representing the range of lithologies, grain size, colors, and degree of weathering. These samples were progressively demagnetized in as many as eight steps. Following the determination of generally stable intervals and coherent directions of magnetization in pilot collec-

tions, the remaining samples were demagnetized in one or two steps, chosen to intersect the midpoint of the range of stability. Samples that did not fully respond to these steps were then progressively demagnetized. Mean locality directions were calculated at demagnetization steps within the range of magnetic stability that gave minimum dispersion of directions, supported by evaluations on orthogonal demagnetization diagrams.

The measurements done in the GSC laboratory involved subjecting all specimens to 8–15 demagnetizing steps. Directions were then determined by using principal component analysis (Kirschvink, 1980). There is no recognizable difference in the quality of measurements from the two laboratories. Example demagnetization plots, taken from both laboratories, are given in Figure 2.

With a few notable exceptions, the collection is characterized by simple magnetizations. Usually, a low-temperature overprint, arising from weathering and alteration or acquired viscously in the present field, is removed by 500 °C. Above this temperature, the characteristic remanent magnetization decays linearly with little deviation to the origin. With demagnetization behavior like this, single-point determinations commonly render the same remanence directions as fitting lines. Hence results of our earlier studies in the Belt-Purcell Supergroup of Montana are not procedurally obsolete and are as reliable as the more recent ones. The same polarities, directions, and demagnetization characteristics were observed by both laboratories.

RESULTS

Most samples were taken from fine-grained red beds. Polished thin sections of red beds generally reveal fresh specularite as well as pervasive red hematite pigment. Detrital specularite grains may contain specks of red hematite, but alteration halos of red hematite around individual specularite grains characteristically are lacking. The red hematite within such grains thus formed before deposition, presumably in the source terrane and/or during transport. At most outcrops, color variations are commonly stratiform in fine detail, evident even in rip-up clasts of local derivation. Additionally, colors of mudstone pebbles and fragments are intrinsic to each fragment, and commonly differ from colors of enclosing strata. This circumstance argues for a penecontemporaneous reddening, lamina by lamina and bed by bed, during the course of deposition. One diagnostic feature used to evaluate the freshness of the rock was the presence of crisp and apparently undegraded ''freckles'' (disseminated reduction spots) in otherwise thoroughly oxidized, hematite-bearing rock.

We report new results from 2700 samples gathered from 93 localities (Table 1, Fig. 3). We only report results from localities at which the magnetization is considered to be original or early diagenetic. These results are described for each formation or member in turn from the top down. This approach allows us to present and establish the validity of the paleomagnetic data that come from the higher formations. We then describe and discuss an interesting remagnetization problem in the lower formations that can be attributed to early deep burial.

Formation-level mean directions (Table 3) do not include localities with poorly defined means ($\alpha_{95} > 15°$) or localities that have undergone remagnetization or large vertical-axis rotations (as noted in Table 1). We observe that the directional dispersion of each formation is greatly reduced after correcting for bedding tilt, indicating that the magnetizations predate deformation and tilting. Rigorous application of the fold test is given in Table 3, where we record the degree of untilting that results in optimal concentrations of directions (Watson and Enkin, 1993). Except for a couple of cases that we discuss subsequently, optimal concentration is never found significantly different from 100% bedding correction, the necessary condition for a positive fold test.

Strata Above Mount Shields Formation

Unit 9: Pilcher Quartzite, Garnet Range Formation, and Libby Formation

Across most of the basin, green quartzite and argillite of the Garnet Range and Libby Formations mark the top of the Belt-Purcell Supergroup, and a regional unconformity separates the Belt-Purcell from overlying lower Paleozoic strata. In the Missoula area, the Garnet Range grades upward into purple crossbedded sandstone of the Pilcher Quartzite. At some exposures, the Pilcher was found to contain stable hematite remanences and coherent directions. In order to have enough localities to produce an average direction, results from the Pilcher Quartzite, Garnet Range Formation, and Libby Formation are grouped together.

In these formations, the reverse-polarity characteristic component is isolated above 590 °C with >50% of the total remanence remaining (Fig. 2, A and B). The high unblocking temperatures are typical of remanence carried by detrital specularite, which usually holds a very accurate depositional remanent magnetization (Elston and Purucker, 1979; Purucker et al., 1980; Bressler and Elston, 1980). An original Wisherd Ridge sampling of the Pilcher reported in Elston and Bressler (1980) was doubled with additional sampling at Lockwood Point (PQlp). The locality mean directions are well clustered except for a single outlier—the Garnet Range Formation at Flint Creek (GRfc), which has a similar inclination to the others but a notable declination difference indicating counterclockwise (CCW) vertical-axis rotation (Fig. 3). Despite the coherence of the other four localities, their small number and their proximity to major structures that could cause vertical-axis rotations make this mean direction the least reliable of the study.

Unit 8: McNamara Formation (Correlated to Kintla Formation Member D and Roosville Formation)

Red beds are found near the base and top of the McNamara Formation with gray beds in between. As shown in Figure 2C, most of the remanence is held by specular hematite with unblocking temperatures very near 670 °C.

More than in any other formation, mean locality directions in the McNamara Formation have smeared declinations but constant inclination, indicating relative vertical-axis rotations of $\leq 50°$ (Fig. 3). We calculate an average direction from all these localities, because they are well distributed around the basin and rotations are assumed (to first order) to be random.

Normal and reversed directions for the McNamara Formation are close to antiparallel ($167° \pm 9°$). A polarity zonation for the McNamara has been compiled from widely separated partial sections. Reverse polarity characterizes the upper half of the McNamara. Together with the Pilcher Quartzite, Garnet Range Formation, and Libby Formation, we identify this constant polarity period as the ''upper reversed zone'' (Fig. 4). An interval of mixed polarity (''upper mixed zone'') is found at three localities (MCwtc, MCwsc, and the top of the MCsb section), lying above the normal interval in the lower McNamara. The lower 200 m at the Spotted Bear locality (MCsb) has normal polarity, marking the top of the ''upper normal zone.''

Unit 7: Bonner Quartzite (Correlated to Kintla Formation Member C, and Phillips Formation)

The Bonner Formation is a widespread, coarse-grained, mica-bearing, purplish red-bed sandstone. Its remanence is typically very

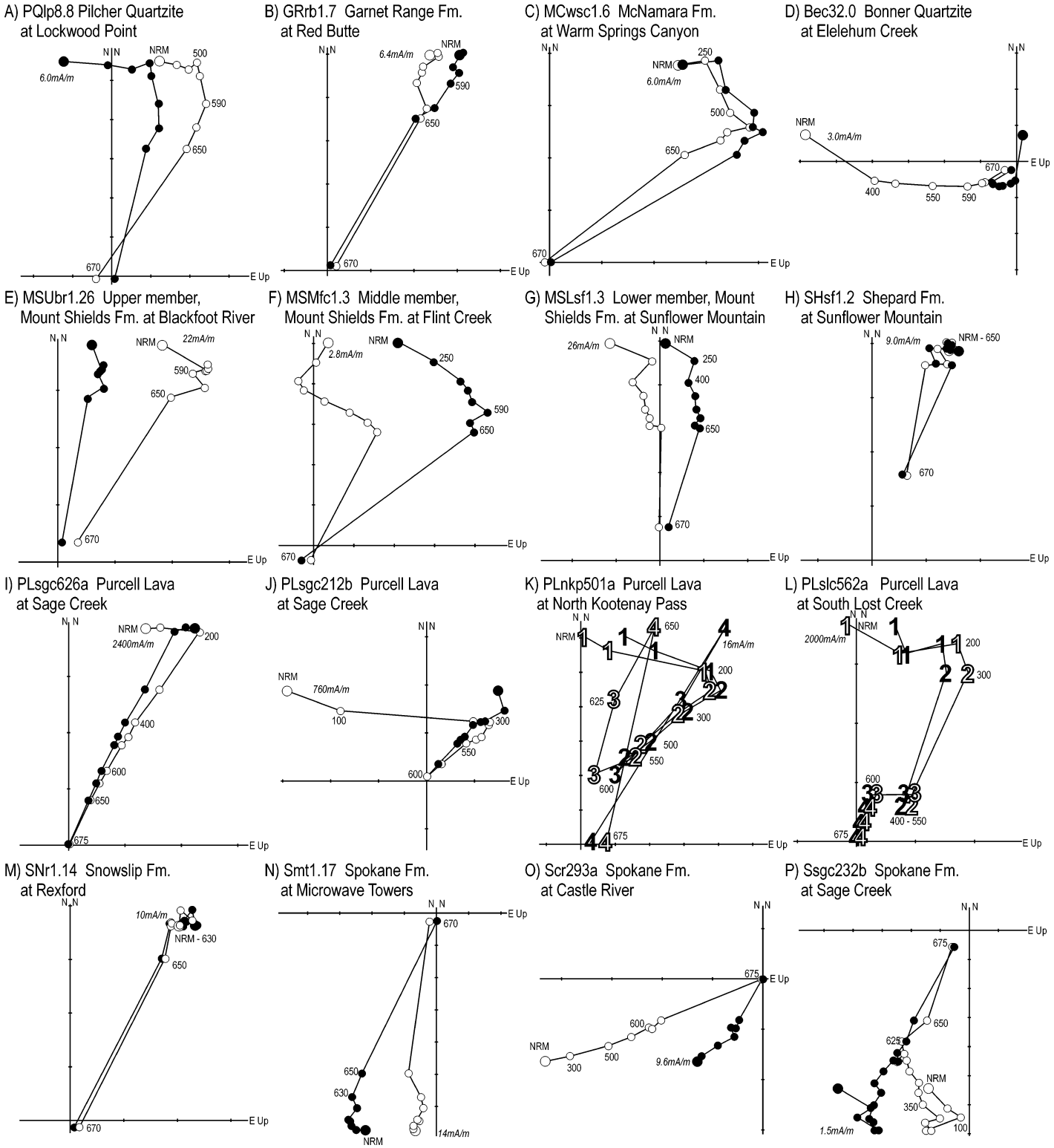

Figure 2. Representative demagnetization behaviors from each formation. The horizontal (vertical) projection is marked with filled (open) circles. Thermal demagnetization steps are labeled in °C. Descriptions of individual specimen behavior are given in the text. Usually the magnetization is dominated by hematite with unblocking temperatures between 600 and 675 °C. In K and L, the points corresponding to four components are labeled.

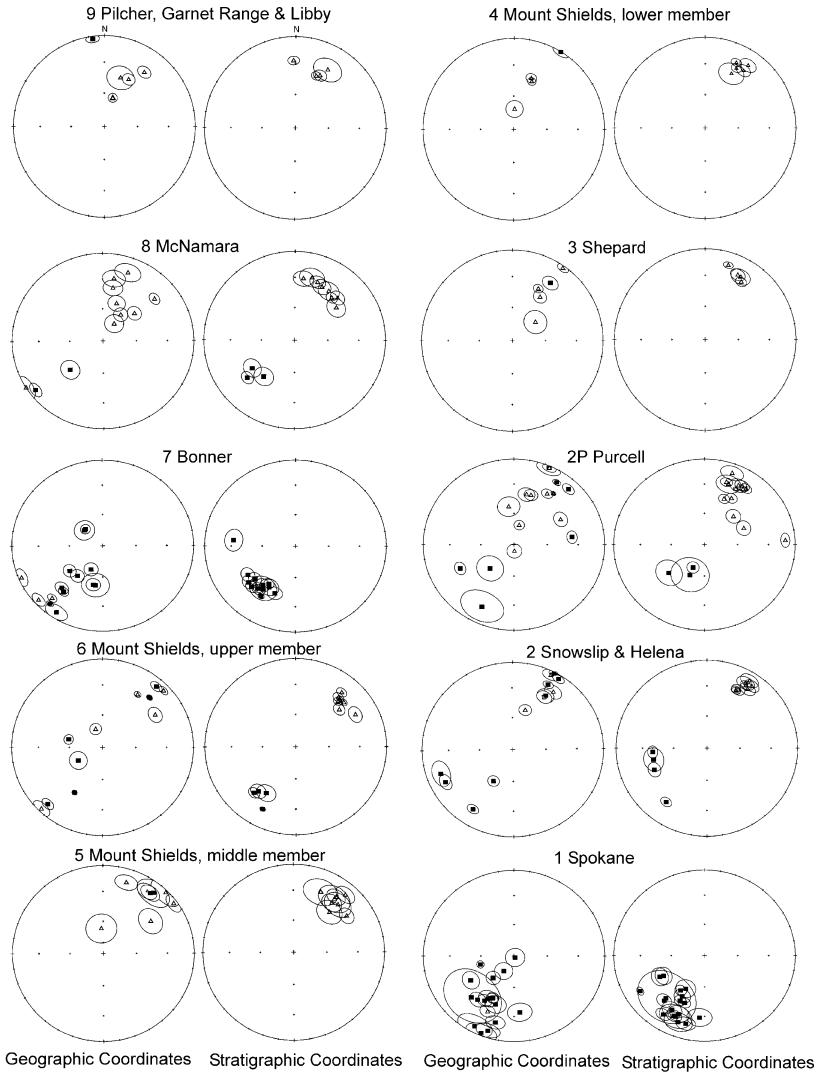

Figure 3. Stereographs of locality means by formation and magnetostratigraphic unit (numbers). Data in lower (upper) hemisphere marked by squares (triangles), and ellipses mark the 95% confidence intervals. For each formation, the directions are best concentrated after stratigraphic correction (i.e., plotted ''stratigraphic coordinates''), giving a positive fold test. Directions are often declination streaked, indicating structurally produced relative vertical-axis rotations. In the lower formations, we observe both shallow- and intermediate-inclination directions; the steeper inclinations are interpreted to be overprints acquired during the deposition of the Bonner Quartzite.

hard and uncontaminated, mostly held by single domain specular hematite. In some samples we see a large present-field component (e.g., Fig. 2D). Locality means are well defined, and dispersion is independent of the sediment grain size.

Locality mean directions are very tightly clustered (Fig. 3), except for Schwartz Creek (Bsc), which is also the only locality with mixed polarity. Elsewhere the Bonner is normal and forms the bulk of the ''upper normal zone'' (Fig. 4). The Schwartz Creek locality has a magnetic inclination similar to the rest of the Bonner and is apparently rotated clockwise (CW) by 60° along the south side of the Lewis and Clark structural discontinuity.

Mount Shields Formation (Correlated to Striped Peak, Kintla Formation Members A and B, and Gateway Formation)

The Mount Shields Formation is divided lithologically into three informal members. Significant differences in paleomagnetic directions and polarities were found between these members.

Unit 6: Upper Member of Mount Shields Formation

Demagnetization reveals the typical square-shouldered remanence of single-domain specular hematite (Fig. 2E). A prominent interval of mixed polarity, the ''middle mixed zone'' (Fig. 4), was recorded during deposition of the upper member. Parts of the interval were found at a number of localities. Detailed magnetostratigraphic sampling, carried out mostly on 1–3 m intervals, was undertaken to define the nature and stratigraphic extent of the mixed-polarity interval.

At Blackfoot River (MSUbr), 220 samples were collected over a 130 m section (7 samples were directional outliers). In a 40 m segment of the section, there are 15 polarity chrons, each defined by more than one sample (Fig. 5A). The Blackfoot River directions are antipodal to 2° ± 4°, showing that the components are not contaminated by later remagnetizations.

An overturned and faulted section 5 km west of Alberton, Montana, originally mapped (Wells, 1974) as Snowslip Formation on the basis of lithology, was found to contain two intervals of mixed polarity apparently separated by a fault (Elston and Bressler, 1980). Additional sampling revealed the existence of multiple reversals. One of the faulted overturned sections contained 10 multisample polarity chrons spread across >30 m (Fig. 5B). We therefore proposed to mappers at the USGS that the section be reassigned to the upper member of the Mount Shields Formation on the grounds that the upper member of the Mount Shields contains abundant reversals whereas the Snowslip Formation exhibits only reverse polarity across nearly all of the Belt-Purcell basin. A geologic reevaluation then led to reassignment of these siltstone and sandstone exposures to the upper member of the Mount Shields Formation (Harrison et al., 1986).

Units 5 and 4: Middle and Lower Members of Mount Shields Formation

As in the upper member of the Mount Shields, the stable early magnetization of the middle and lower members is carried by hematite pigment and specularite (e.g., Fig. 2G). However, some sections have been deeply buried and appear darkened and altered. Such rocks characteristically contained a lower-temperature overprint that was demagnetized by 590 °C and presumably carried by magnetite (e.g., Fig. 2F). All localities in the middle and lower members of the Mount Shields exhibit reverse polarity. These members mark the up-

TABLE 3. BELT-PURCELL SUPERGROUP FORMATION MEANS

Formation	Geographic coordinates					Stratigraphic coordinates				Optimal untilt (%)	Pole		
	N	D (°)	I (°)	k	α_{95g} (°)	D (°)	I (°)	k	α_{95s} (°)		lat (°N)	long (°E)	A_{95} (°)
9. Pilcher, Garnet, and Libby	4	26.2	−43.8	24.6	18.9	28.4	−32.5	102.2	9.1	121 ± 22	−19.2	215.3	7.7
8. McNamara	10	38.5	−37.9	8.9	17.1	37.2	−36.6	42.8	7.5	97 ± 7	−13.5	208.3	6.7
7. Bonner	12	219.9	28.5	7.1	17.5	219.8	38.6	85.8	4.7	106 ± 5	−11.3	206.7	4.3
6. Mount Shields, upper member	11	37.9	−17.4	3.3	29.9	41.8	−29.7	74.1	5.3	104 ± 2	−15.6	202.3	4.4
5. Mount Shields, middle member	8	37.9	−14.0	7.2	22.1	39.2	−27.1	60.6	7.2	102 ± 11	−18.2	203.9	5.8
4. Mount Shields, lower member	4	22.0	−39.4	7.2	36.7	26.3	−21.2	116.9	8.5	96 ± 9	−26.1	215.0	6.5
3. Shepard	5	34.2	−24.7	5.5	36.0	29.5	−24.8	121.9	7.0	112 ± 9	−23.2	212.5	5.5
2P. Purcell primary	10	25.0	−23.7	7.0	19.7	26.6	−25.7	64.0	6.1	100 ± 4	−23.6	215.6	4.8
Purcell overprint	5	229.8	50.0	7.3	30.4	223.9	55.8	44.4	11.6	82 ± 10	3.4	210.0	14.1
2. Snowslip	9	29.7	−1.0	9.5	17.6	30.9	−20.6	128.8	4.6	100 ± 6	−24.9	210.2	3.5
Snowslip and Helena overprint	3	239.6	31.0	9.0	43.7	256.7	39.2	117.1	11.4	95 ± 12	8.1	178.5	10.5
1. Spokane primary	8	205.1	19.5	8.1	20.7	206.3	23.7	86.4	6.0	105 ± 7	−24.8	215.5	4.7
Spokane overprint	5	207.0	50.3	13.5	21.6	207.3	46.0	154.0	6.2	117 ± 16	−10.3	219.5	6.3
Spokane primary and overprint	13	205.7	31.7	7.6	16.0	206.6	32.3	35.4	7.1	117 ± 7	−19.8	217.0	6.0

Note: N—Number of localities, D—declination, I—Inclination, k—Fisher precision, α_{95}—95% confidence interval about mean direction, subscript g—geographic coordinates, subscript s—stratigraphic coordinates, Untilt—degree of untilting (± 95% confidence interval) that gives optimal concentration, A_{95}—95% confidence interval about pole. Mean (9) has lower reliablity than the others because of the possibility of vertical-axis rotations.

per end of the ''middle reversed zone'' (Fig. 4).

Strata Below Mount Shields Formation

Unit 3: Shepard Formation (Sheppard in Canada, Correlated to Upper Member of Wallace Formation)

Red beds are rare in the dolomitic Shepard Formation. Buff to pale red pigmented dolomites and argillites locally contain stable, though commonly more scattered remanence directions (Fig. 2H). We include here the site mean reported by Evans et al. (1975) from a study around Mount Gladstone. The formation also lies within the ''middle reversed zone'' (Fig. 4).

Unit 2P: Purcell Lava (Correlated to Nicol Creek Formation)

Basaltic flows of the Purcell Lava occur near the top of the Snowslip Formation and are more abundant in the Canadian part of the basin. Reddened flow tops and microscopically observed hematite pigment combined with a lack of pillows indicate the flows were hematized by exposure to the atmosphere during and shortly after cooling (e.g., Evans et al., 1975). Reddening of the flow tops occurred before deposition of overlying green and red strata. Intrusive bodies and subaqueous flows lack hematite, and these generally retained unreliable records of the paleofield.

Stable magnetizations in the Purcell flows reside mainly in hematite (Fig. 2I). Magnetizations residing in magnetite and occasionally pyrrhotite also were observed (Fig. 2J). At two sites, the rocks contained complicated, yet surprisingly consistent four-component magnetizations. At site PLslc56 (Fig. 2L), (1) the present-field magnetization was eliminated by 300 °C; (2) a component in the Belt-Purcell direction held by pyrrhotite was removed by 400 °C; (3) then a steep component held by magnetite remained up to ~<575 °C; and (4) finally a primary magnetization residing in hematite pigment and specularite remained up to 675 °C. At site PLnkp50 (Fig. 2K), (1) a present-field overprint was removed by 300 °C; (2) then we observed a scattered reverse-polarity Belt-Purcell direction probably held by magnetite and hematite pigment up to 600 °C; (3) followed by a scattered normal-polarity Belt-Purcell direction in the moderate to high temperature range of 600° to 650 °C that is due to hematite remanence; and (4) finally a coherent reverse-polarity Belt-Purcell direction was maintained up to 675 °C. The normal-polarity overprint could record a diagenetic event that altered (secondarily oxidized) original magnetite, possibly during early burial.

Remanence directions in the Purcell flows are more dispersed than directions from the enclosing red-bed strata (Fig. 3). One source of dispersion may be that magnetite, more strongly magnetized than syngenetically formed hematite pigment and specularite in the flows, may have preserved spot readings of geomagnetic secular variation while passing through its blocking temperature range. In contrast, early chemical remanent magnetizations within the flows and in oxidized flow tops, as well as detrital remanence in enclosing red sediments, provided slightly more extended, but still brief time averages of the field. A second source for the increased dispersion might be complex unexplained interactions between magnetizations acquired at different times in different minerals during cooling and early hematite formation. Finally, secondary overprinting arising from burial or tectonic events also may have affected dispersion of directions.

The distribution of Purcell directions after stratigraphic correction is not circularly symmetrical about a single mode, as expected for secular variation, but rather falls into two main groups. One group has a shallow-up north-northeast direction. Such remanences have unblocking temperatures of >650 °C and are dominantly carried by single-domain hematite. The other group has steeper inclinations and CW-rotated declinations; their remanences usually are carried by combinations of magnetite and hematite having unblocking temperatures of <600 °C. We argue that the shallow directions are primary, whereas the steeper directions are secondary and reflect overprinting during the later part of the Belt-Purcell basin deposition.

At several localities (PLbc, PLr, PLsgc, PLslc, PLtpc) we found sites exhibiting both direction groups. For example, at Sage Creek, one site (PLsgc62) by the creek has the shallow inclination carried by hematite, whereas three sites on the road 40 m above have steeper inclinations held by pyrrhotite and magnetite (e.g., Fig. 2J). The four-component site (PLslc56) at the South Lost Creek locality (already described) has a steep direction held in its 400–600 °C component, which we interpret to be an overprint. The shallow primary direction is revealed at higher temperatures. At Bobtail Creek (PLbc) and Rexford (PLr), reverse-polarity directions fit the shallow population, whereas normal-polarity directions are scattered and far from antipodal (151° and 145°, respectively), indicating they are secondary overprints.

The shallow group of directions strongly

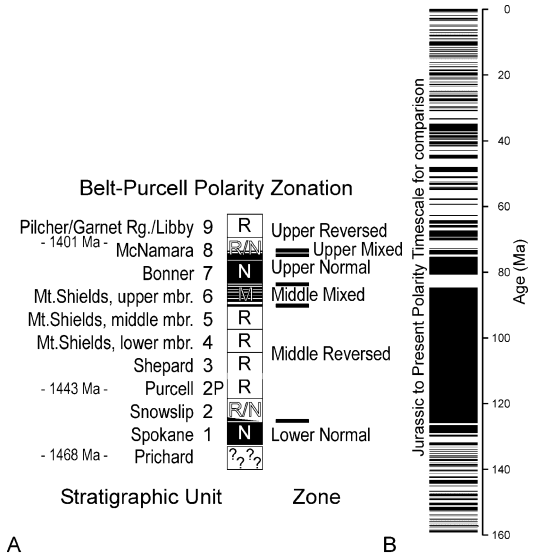

Figure 4. (A) The Belt-Purcell polarity stratigraphy—normal (reverse) polarity indicated by black (white). Except for the upper member of the Mount Shields Formation and lower McNamara, the formations display a single polarity transition. (B) For comparison, the Jurassic to present polarity time scale (from Harland et al., 1990) is plotted on the right at what is suggested to be the same scale. Given a duration of 50–100 m.y. and no recognized major unconformities, the Belt-Purcell reversal frequency is lower than the frequency for most parts of the past 200 m.y. We propose that the middle reversed zone marks a long superchron comparable to the Cretaceous long normal superchron, ~40 m.y. in length.

passes the tilt test (Table 3). The close similarity of directions in the Purcell Lava to those from the enclosing Snowslip and overlying Shepard Formation attests to their primary nature. We ascribe magnetizations in the steep group of directions to burial or hydrothermal alteration occurring during the later part of Belt basin deposition when the geomagnetic field was steeper (Fig. 3).

Unit 2: Snowslip and Helena Formations (Correlated to Middle Member of the Wallace Formation and Siyeh Formation)

The Snowslip Formation marks the onset of shallow-water deposition of the Missoula Group, accumulating above somewhat deeper-water Middle Belt Carbonate of the Helena Formation. Stable remanences and tightly clustered directions were obtained from rare red-bed intervals near the base of the Snowslip (Fig. 2M). The strata are dominantly reverse polarity. At the very base of the formation, normal polarity was observed at Poorman Creek (SNpc), whereas reverse polarity was observed at Ousel Creek (SNoc). The stratigraphic position of the polarity switch marks a south to north transgression of the Snowslip across a regional unconformity above the Helena Formation. Normal polarity was consistently observed in samples from the gray Helena Formation collected from its easternmost exposures at Dearborn Canyon. This polarity transition is the base of the ''middle reversed zone'' and the top of the ''lower normal zone'' (Fig. 4).

Anomalous directions were obtained from exposures of atypical purple beds in (1) an attenuated Snowslip Formation at Trail Gulch (SNtg), (2) purplish to pale-red beds in the basal Snowslip at the southern end of the Flint Creek section (SNfcl), and (3) pale-purple beds of the Helena Formation at Trail Gulch (Htg). These localities have remanences with normal polarity, relatively steep inclinations, and CW-rotated declinations. As with the Purcell flows, we consider these anomalous directions to reflect postdepositional alteration and overprinting. Buff dolomites common to the Helena Formation contain weak, incoherent remanences.

Unit 1: Spokane Formation (Correlated to Grinnell Formation)

The widespread bright red rocks of the Spokane Formation are conspicuous paleomagnetic targets. The beds, which crop out in the eastern part of the basin, contain single-component remanences that unblock in the range of ~500 to 675 °C (e.g., Fig. 2, N and O) and reside in primary specular and early-pigment hematite.

At some places, such as at Sage Creek (Ssgc), the Spokane Formation exhibits a posttilting reverse-polarity Cretaceous overprint direction (e.g., Fig. 2P). Such an overprint reflects the generation of secondary magnetite as a consequence of heating, possibly arising from deep burial. Nonetheless, some of the original hematite magnetization is retained.

Although locality mean directions for the Spokane are similar to normal-polarity directions from other formations of the Belt-Purcell, there is considerably more complexity. The distribution of directions is bimodal (Fig. 6), similar to the shallow-and steep-inclination groups observed in the Purcell Lava and Snowslip red beds. For each group, there are localities that have similar inclinations but discordant declinations (Ss, Sac, Slpp); vertical-axis rotations that postdate development of the two groups are indicated. When we analyze the unrotated bimodal locality directions as a single group, a maximum concentration of directions is found when tectonic tilting is overcorrected by 117% ± 7%. This degree of untilting is impossible for an original magnetization. If only shallow-inclination localities are selected, the maximum concentration occurs on 105% ± 7% untilting, indicating a pretilting magnetization. Directions from the steep-inclination localities are more dispersed (maximum concentration occurs at 117% ± 16%); these directions also are probably (but less definitively) pretilting.

The Spokane direction data from Glacier National Park (Sgnp77), sampled by Vitorello and Van der Voo (1977), fit the steep inclination group, and they weakly pass the fold test (optimal untilting at 121% ± 24%). These rocks also contain an intermediate-temperature magnetization that exhibits a west-declination shallow, downward-inclination direction. Magnetizations of the Spokane Formation from the Rocky Mountain Trench in the central Belt-Purcell basin (e.g., Ss, Slb) have the steeper inclinations. The rocks here are not bright red as elsewhere, but rather are dark gray to purplish gray in color and respond to alternating field demagnetization. These rocks were buried to >10 km, and much of their magnetization appears to be carried by magnetite developed during deep burial. Geologic mapping in the region of the overprinted Spokane in the eastern Belt-Purcell basin indicates deep burial (~5 km) during Bonner time (C.A. Wallace, 1984, personal commun.). Such burial apparently was

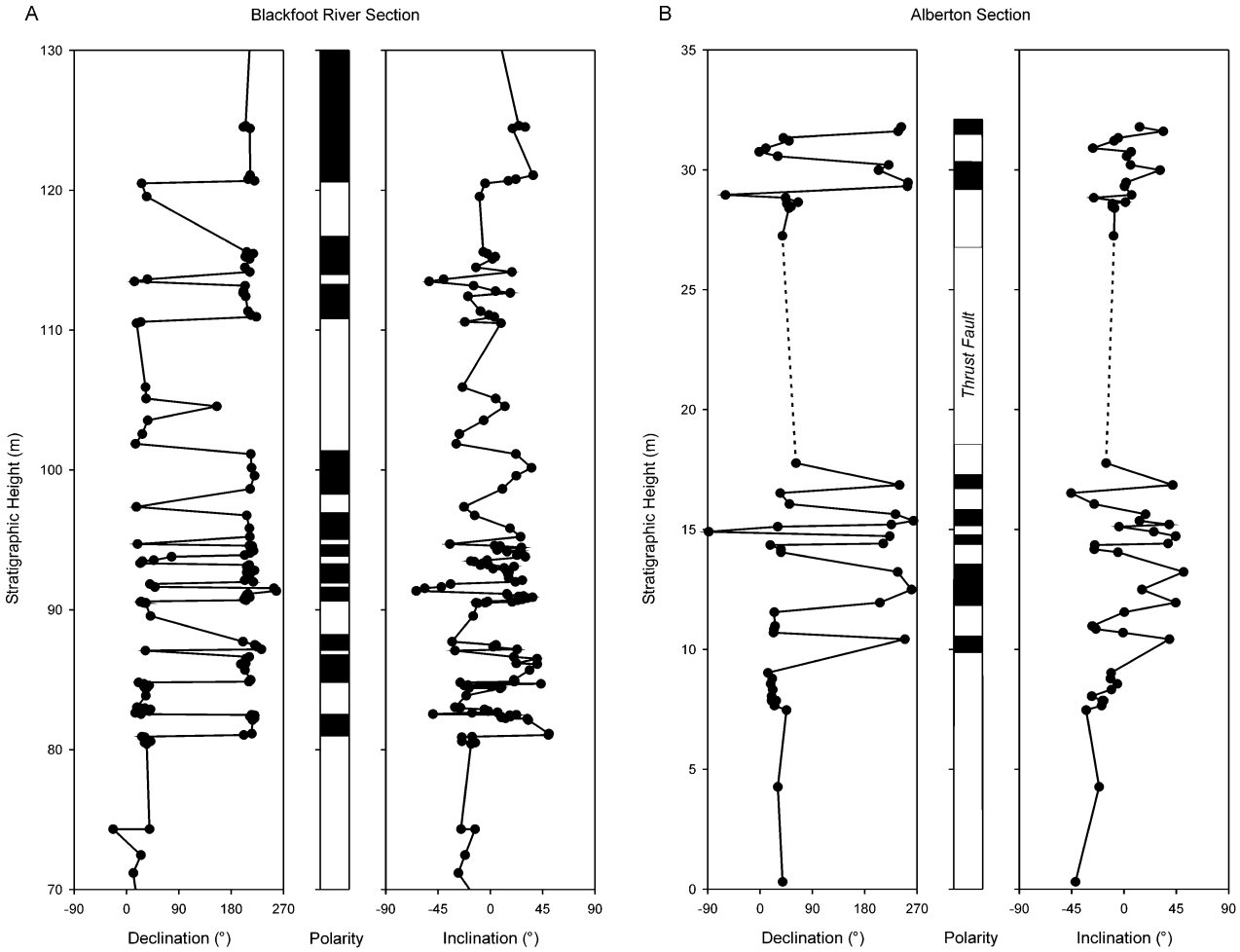

Figure 5. Magnetostratigraphic columns of two sections of the upper member of the Mount Shields Formation. These are the only sections found that contained fairly complete records exhibiting abundant rapid reversals definable on a 1–3 m scale. The fine-scale nature of reversal behavior and its regional correlation strongly indicate paleomagnetic stability and early, accurate recording of the ambient field.

responsible for partial remagnetization of the Spokane.

Prichard Formation and Moyie Sills (Correlated to Aldridge, Appekunny, and Altyn Formations)

Magnetizations of the Lower Belt Group (mainly Prichard Formation turbidites and contemporaneous Moyie sills) are weak and incoherent. The scattered directions are nonreproducible and do not pass the fold test. Symons and Timmons (1992) reported results from 57 sites, but also found directions that fail the fold test.

DISCUSSION

Reliability and Primary Nature of the Paleomagnetic Results

For the following eight reasons, we conclude the magnetization of much of the Belt-Purcell Supergroup accurately reflects the ambient field during the time of deposition. (1) The dominant magnetic remanence carriers are detrital specularite and hematite pigment, the most stable of all magnetic minerals. Macroscopic and microscopic evidence shows that the hematite is original and accumulated or formed during the depositional and lithification process. Progressive thermal demagnetization commonly reveals a single component of magnetization exhibiting unblocking temperatures approaching 675 °C. This outcome explains why early paleomagnetic work on these rocks gave results comparable to those obtained by using modern methods. (2) Rocks that show no evidence of secondary alteration are not magnetically overprinted. (3) Taken either as a whole or formation by formation, the magnetization directions have optimal concentrations at ~100% untilting (Table 3), which indicates that the directions pass the fold test (Watson and Enkin, 1993). (4) Magnetic polarities are stratigraphically consistent, both in fine detail and regionally across the basin. (5) Normal- and reverse-polarity directions are antipodal, giving a positive reversal test. (6) The remanent directions (south-southwest shallow down or north-northeast shallow up) are distinctive and are not seen in North American rocks of any younger age; thus these directions cannot be ascribed to some later overprinting process. (7) The fact that the same directions are observed in interbedded volcanic flows and in sedimentary strata of widely ranging grain size demonstrates that inclination errors arising through depositional or compaction processes are negligible. (8) A smooth progressive evolution of coherent directions occurs across the Belt-Purcell stratigraphic section: the lower formations have shallower inclinations and lower declinations than the upper formations. Stratigraphically neighboring directions do not differ significantly; however, directions and poles from

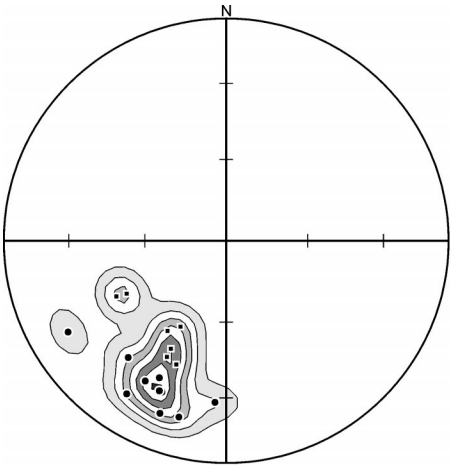

Figure 6. Spokane Formation distribution of locality mean directions. Contours are every 0.5 using Gaussian counting with Fisher precision k = 100. The main cluster is bimodal, displaying a shallow primary remanence (solid circles) and a steeper overprinted remanence (solid squares). Large declination deviations result from vertical-axis rotations.

high in the section are significantly different from lower directions and poles, up to a difference of 21° ± 6°.

We can thus confidently say that the ancient ambient field direction was progressively and accurately recorded during accumulation of strata across the Belt-Purcell basin. The directions have allowed construction of an accurate, high-resolution, stratigraphically controlled apparent polar wander path (Fig. 7).

The lower formations (Spokane Formation, Snowslip Formation, and Purcell Lava) contain two directional groups of magnetizations that exhibit both shallow and steeper inclinations. When these locality-mean directions are analyzed together, they have optimal concentrations significantly above 100% untilting. This absurd result indicates that we are not looking at a single population of coherent directions. In contrast, the shallow-inclination group alone has optimal concentration at 100% untilting and thus passes the tilt test. Localities that contain the steeper inclinations are commonly from parts of the basin that have undergone deeper burial (e.g., Wolf Creek localities in the eastern Belt-Purcell basin, locally buried to a depth of ~5 km by deposition of the Bonner Quartzite). At one such locality, the steeper direction was removed by 600 °C thermal demagnetization, and the shallow direction was revealed at higher demagnetization temperatures. We therefore interpret the shallow-inclination directions in the lower formations to be primary and the steeper-inclination directions to be the product of burial remagnetization. The steep-inclination secondary directions are similar to primary directions found in the upper member of the Mount Shields Formation and Bonner Quartzite; both are unlike directions derived from younger rocks of the North American craton. We therefore interpret that remagnetization of parts of the Purcell Lava, and Snowslip and Spokane Formations below the Missoula Group occurred during tectonic events responsible for deposition of the flood of sand that made up the Bonner Quartzite.

Figure 7. The Belt-Purcell apparent polar wander path; poles are marked as triangles with their 95% confidence intervals. The basin is indicated by the white area in North America. The poles are numbered as in Table 3. The pole for the topmost formations gathered together to calculate pole 9 is less reliable than the rest. The poles trace out a simple path, with a ~10° jump in paleolatitude occurring between the time of deposition of the middle member of the Mount Shields Formation and deposition of the Bonner Quartzite (pole 7). Nonetheless, to first order, the poles mark a standstill in North America's position during the period of Belt-Purcell deposition.

The stability and high coercivity of the hematite magnetization contrast markedly with the tendency for magnetite to be more readily remagnetized by postdepositional events. In magnetite-bearing Paleozoic carbonates that overlie the Belt-Purcell Supergroup in Canada, detailed study (Enkin et al., 2000) has not revealed a single instance where the original magnetization was retained. In contrast, a hematite-bearing Devonian anhydrite horizon from an oil-well core collected in southwest Alberta was found to retain a Devonian shallow inclination (Lewchuk et al., 1996). Similarly, Belt-Purcell carbonates and black, gray, or green clastic rocks (which could have magnetite as the principal carrier) yielded weak and incoherent magnetizations. In some samples we recognized a secondary Cretaceous direction in such rocks. As a class, rocks from this region and lacking a hematite component have retained no record of the paleofield in which they were deposited or formed.

The Apparent Polar Wander Path (APWP) of the Belt-Purcell Supergroup

Formation mean paleomagnetic poles (Table 3) are generated by averaging all localities (after inverting reverse-polarity directions). We use only apparently primary magnetizations with 95% confidence limits below 15° and <15° vertical-axis rotation relative to the rest of the collection. These poles (Fig. 7) plot in the area of the South Pacific.

Paleogeographically, the Belt-Purcell apparent polar wander path implies little plate motion between the deposition of the Spokane Formation and the deposition the lower member of the Mount Shields Formation, followed by a CW rotation of 15° during the deposition of the upper member of the Mount Shields Formation. At that time, the basin and perhaps the continent underwent an abrupt and significant change in direction of movement and sense of rotation. The paleolatitude increased by 6° between the time of deposition of the upper member of the Mount Shields Formation and that of the Bonner Quartzite. The final phase of Belt-Purcell motion is not as well defined because we have sampled few localities of the topmost formations and these come from sites that may have undergone significant vertical-axis rotation, but at which the paleolatitude has remained constant. There appears to be no significant break in deposition between the McNamara Formation and the topmost formations.

We hypothesize that the change in motion around the time of deposition of the Bonner Quartzite is causally connected to the change in sedimentation to coarse-grained quartz sand. This sediment presumably was derived from an uplift event, informally named the ''Bonner disturbance'' (Elston, 1991; Link et al., 1993, p. 572). Geologic mapping in the region of the paleomagnetically overprinted rocks of the Spokane Formation indicates their deep burial (~5 km) during deposition of the Bonner sand (C.A. Wallace, 1984, personal commun.). Such burial most likely served to partially remagnetize the Spokane Formation in a locally deeper region of the eastern Belt-Purcell basin.

Middle Proterozoic Laurentian Apparent Polar Wander Path

Laurentia (Precambrian North America) was formed during Early Proterozoic accretion events (Hoffman, 1989), and its various older subcratons have distinct paleomagnetic poles. There are no reliable poles from the period 1750–1500 Ma, marking a large break that precedes the APWP shown in Figure 8. Forward in time from 1500 Ma and continuing to the Phanerozoic, the APWP is established reliably enough to be confident of the polarity of the Belt-Purcell directions. For the period ca. 1500 to ca. 1300 Ma, most poles have come from the anorogenic ''Elsonian'' intrusions of Labrador. Most Elsonian poles are scattered about ~210°E, near the equator (Fig. 8).

The Belt-Purcell poles have a similar longitude, but are concentrated ~20° farther south. This different location might indicate a subsequent displacement of ~2000 km of the Belt-Purcell basin with respect to the rest of the Laurentia. However, the Belt-Purcell overlies North American basement (Ross et al., 1991; Winston, 1986, 1989), and structural discontinuities that could accommodate such large lateral displacements within the Laurentian craton have not been identified.

Until recently, the only paleomagnetic poles lying near the Belt-Purcell APWP came from the Sibley Group of Ontario, underlying Keweenawan deposits on the north shore of Lake Superior (Robertson, 1973). The age of the Sibley Group is poorly determined, controlled only by a 1339 Ma sedimentary-rock Rb-Sr age (Franklin, 1978); recently, xenoliths of lower Sibley Group? rocks have been found in a 1537 Ma granite (J.M. Franklin, 2000, personal commun.). Paleomagnetically, reverse- and normal-polarity poles for the Sibley Group closely parallel those of the Belt-Purcell Supergroup; a reverse polarity from the lower Sibley Group (K1 in Fig. 8) is similar to Ravalli and lower Missoula Group poles (B1 to B4), and a normal-polarity pole from the upper Sibley Group (K2) is similar to upper Missoula Group poles (B7 and B8). Results from the 1433 ± 3 Electra Lake Gabbro in Colorado (Harlan and Geissman, 1998; pole A6 in Fig. 8) now confirm that at least one pole of appropriate age from igneous rocks elsewhere in Laurentia falls in the region of the Belt-Purcell poles. The Belt-Purcell poles therefore establish the southern position as a time of ''standstill'' on the Laurentian APWP between ca. 1450 and ca. 1400 Ma.

Two other Elsonian-age poles have recently been restudied, the Laramie Anorthosite and Sherman Granite (Harlan et al., 1994; pole A5), and the St. Francois Volcanics (Stuckey et al., 1999; J.G. Meert, 2000, personal commun.; pole A2). Both studies show poles lying well south of the equator and close to the Belt-Purcell APWP.

The controversy concerning differences between the Belt-Purcell poles and the Elsonian poles was predicated on the idea that Belt-Purcell deposition overlapped in time with the Elsonian intrusions (e.g., Irving and Wynne, 1991). In contrast, we propose that the Belt-Purcell poles represent a relatively short period that fits in age between two sets of Elsonian poles. The older poles (A1–A6 in Fig. 8) trace a southward-descending path trending toward the Belt-Purcell near-standstill. Then the poles follow a loosely defined northward-ascending path represented by the later Elsonian poles (C1–C6 in Fig. 8). New radiometric work on these intrusions has shown that several earlier-reported dates were too great. Murthy's (1978) pole for the Nain Anorthosite at Paul Island (C-3), originally dated at 1418 Ma by Rb/Sr (Barton, 1974), now has a zircon age of 1319 Ma (Hamilton et al., 1994) and a still younger Ar-Ar (plagioclase) age of 1171 Ma (Yu and Morse, 1993). The Seal Lake Group (C-1) (Roy and Fahrig, 1973; Park and Roy, 1979) had a Rb-Sr age of 1350 ± 92 Ma (Wanless and Loveridge, 1978), but more recently baddeleyite and zircon ages of 1250 and 1224 Ma have been determined (Romer et al., 1995). The broad similarity of the early and late Elsonian poles and ages as well as the large uncertainties in the Belt-Purcell ages made the Belt-Purcell poles seem aberrant. However, the poles for the Belt-Purcell in fact trace out a large part of the base of an intervening smooth hairpin turn.

The Belt-Purcell APWP approaches but does not clearly overlap the polar path for the Grand Canyon Supergroup (Elston and Scott, 1973; Elston and Grommé, 1974; Elston and McKee, 1982; Elston, 1989; Link et al., 1993; given here in Table 4 and Fig. 8). Indeed, results from the lowest formations of the Grand Canyon Supergroup form a westward and then northward track that starts near the western limit of the Belt-Purcell loop. Paleomagnetically, we can state that the lower Bass Limestone and overlying lower member of the Hakatai Shale of the Grand Canyon succession accumulated significantly after deposition of the Belt-Purcell Supergroup. We also note that unconformities separate the widely spaced poles for the lower Hakatai, upper Hakatai, and Shinumo Quartzite. Above this stratal level, deposition occurred without major break to the top of the Unkar Group.

There are no isotopic dates from the lower part of the Grand Canyon Supergroup; the only isotopically dated formation is the 1070 ± 70 Ma (whole-rock Rb-Sr) Cardenas Basalt at the top of the Unkar Group (Elston and McKee, 1982). Timmons et al. (2001) reported $^{40}Ar/^{39}Ar$ ages of between 1350 and 1200 Ma on K-feldspars (200 °C closure temperature) from the underlying metamorphic suite. They interpret the 1200 Ma age to be an upper bound on the start

Figure 8. Middle Proterozoic paleomagnetic poles and apparent polar wander path for Laurentia. Solid (open) symbols have normal (reverse) polarity, symbols divided in half vertically have mixed polarity, and those divided in half horizontally indicate the general sense of a polarity switch. The poles are grouped by letter and numbered from oldest to youngest. The A poles (squares) are from pre–Belt-Purcell intrusions and strata (A1—Croker Island pluton, A2—St. Francois Volcanics, A3—Michikamau Anorthosite, A4—Harp Lake Anorthosite, A5—Laramie Anorthosite Complex and Sherman Granite, and A6—Electra Lake Gabbro), compiled by Harlan et al. (1994) and Buchan et al. (2000). The B poles (diamonds; sequence tied by lines) are from the Belt-Purcell Supergroup (B1—Spokane Formation, B2—Snowslip Formation, B2P—Purcell Lava, B3—Shepard Formation, B4—lower member of the Mount Shields Formation, B5—middle member of the Mount Shields Formation, B6—upper member of the Mount Shields Formation, B7—Bonner Quartzite, B8—McNamara Formation, B8—Pilcher Quartzite, and Garnet Range and Libby Formations), from this paper (see Table 3). The C poles (up-pointing triangles) are from post–Belt-Purcell intrusions and strata, excluding Grand Canyon and Keweenawan data (C1—Seal Lake Group Red Beds, C2—Mistastin pluton, C3—Nain Anorthosite, C4—Coppermine River Group, C5—MacKenzie dikes, C6—Sudbury dikes, C7—Arizona diabase sheets), compiled by Harlan et al. (1994), and Buchan et al. (2000). The G poles (circles; sequence tied by lines, dashed across unconformities) are from the Grand Canyon Supergroup (G1—Bass Limestone, G2 and G3—Hakatai Shale (lower and upper members, respectively), G4—Shinumo Quartzite, G5–G11—Dox Sandstone (seven stratigraphic collections from the lower to upper members), G12—Cardenas Basalt, G13 and G14—Nankoweap Formation, lower and upper members), reported by Elston in Link et al. (1993) and given in Table 4. The K poles (down-pointing triangles) are from the Keweenawan Supergroup (K1 and K2—Sibley Group (lower and upper), K3—lower Powder Mill Volcanics, K4—Michipicoten Island Volcanics, K5—Clay Howells Carbonatite Complex, K6—Portage Lake Volcanics, K7—Firesand Carbonatite, K8—Osler Group (normal polarity), K9—Logan dikes, K10—upper part of North Shore Volcanic Group, K11—Chipman Lake Carbonatite, K12—Mamainse Point Volcanics, K13—Seabrook Lake Carbonatite, K14—Copper Harbour Conglomerate, K15—Fond du Lac Sandstone, K16—Nonesuch Shale, K17—Eileen Sandstone, K18—Middle River Sandstone, K19—Freda Sandstone, K20—Jacobsville Sandstone, K21—Chequamegon Sandstone), compiled by Halls and Pesonen (1982), Harlan et al. (1994), and Weil et al. (1998). Because of the close correspondence of the normal-polarity poles from the Grand Canyon Supergroup, the Keweenawan Supergroup, and the Arizona diabase sheets and because of the observation of highly asymmetric reversals in these regions at the same places on both polar paths (K3 ≅ G4; K8–K12 ≅ G7–G8 ≅ C7), only normal-polarity poles have been used to define the Unkar-Keweenawan loop for the interval ca. 1150–1050 Ma. Note that this includes using the lower Powder Mill Volcanics pole (K3), which lies close to the pole of the Shinumo Quartzite (G4) and is included as part of the ascending path of the loop, rather than representing a remagnetization during the time of the descending path (e.g., Palmer and Halls, 1986).

of Grand Canyon Supergroup deposition. Alternatively, the basement ages could be interpreted to mark low-level heating to ~200 °C, far too low to affect the hematite-carried magnetic remanence of the overlying strata.

To accommodate then-existing isotopic ages and as a compromise between wide differences in geologic concepts that existed at the time, Link et al. (1993) estimated that the end of Belt-Purcell deposition and the beginning of Grand Canyon deposition occurred at ca. 1250 Ma. Given the new radiometric constraints and paleomagnetic inferences on Belt-Purcell duration discussed in this paper, we conclude that the end of Belt-Purcell deposition goes back close to 1400 Ma. An ~200 m.y. window, extending from ca. 1200 to ca. 1400 Ma, thus allows the Bass Limestone and the lower member of the Hakatai Shale to have been deposited much earlier than previously postulated. The poles for the Bass, lower Hakatai, upper Hakatai, and Shinumo form a zigzag path that is interpreted to reflect incremental movement of the craton. The movements presumably were punctuated by episodes of uplift and erosion, represented by unconformities in the stratigraphic record. The unconformities, in turn, can

TABLE 4. GRAND CANYON SUPERGROUP FORMATION MEANS

Unit	*N*	*D* (°)	*I* (°)	*k*	α_{95} (°)	Pole lat (°N)	Pole long (°E)	A_{95} (°)	N/R	Comment
G17: Sixtymile Formation	30	276.9	−29.5	25.8	5.3	−3.9	142.4	6.3	R	
G16: Kwagunt Formation	14	269.0	−9.0	26.5	7.9	1.9	162.4	5.6	R	
G15: Galeros Formation	50	257.3	−6.5	70.9	2.4	−12.2	163.0	1.7	N	
G14: Nankoweap Formation, upper member	87	261.8	−4.7	20.6	3.4	−8.0	161.1	2.4	NR	
G13: Nankoweap Formation ferruginous zone and lower member	62	264.2	36.7	42.1	2.8	7.4	178.1	2.5	N	
G12: Cardenas Basalt	13	260.9	42.8	53.9	5.7	7.6	183.4	5.5	N	1070 ± 70 Ma. 8 flows and 5 sandstone interbeds
G11: Dox Sandstone, uppermost upper member	37	260.3	30.1	19.9	5.4	1.9	176.9	4.5	N	
G10: Dox Sandstone, upper member	47	282.0	36.9	40.9	3.3	21.4	168.7	3.0	N	
G9: Dox Sandstone, upper middle member	164	287.9	49.0	52.6	1.5	30.6	174.7	1.6	N	Asymmetric reversals
G8: Dox Sandstone, upper middle member (lower part)	123	295.1	52.0	36.5	2.1	37.3	174.3	2.4	N	
G7: Dox Sandstone, lower middle member (lower part)	129	291.8	57.4	54.0	1.7	36.8	182.1	2.1	N	
G6: Dox Sandstone, uppermost lower member and lower part of lower middle member	73	290.7	54.3	74.8	1.9	34.8	178.9	2.2	N	
G5: Dox Sandstone, upper part of lower member	69	281.9	45.9	42.2	2.7	24.7	174.9	2.8	N	
G4: Shinumo Quartzite, lower middle member and lower part of upper middle member	58	268.2	45.7	49.7	2.7	14.2	181.5	2.7	N	Positive fold test Asymmetric reversals
G3: Hakatai Shale, upper member and parts of middle member	36	249.5	62.8	39.5	3.8	12.0	204.7	5.3	N	Positive fold test Middle member mostly unstable
G2: Hakatai Shale, lower member	27	238.1	23.3	36.4	4.7	−17.1	187.8	3.6	N	Positive fold test
G1: Bass Limestone, upper part	33	232.5	37.9	151.8	2.0	−14.7	197.9	1.8	N	Not including lower part overprinted by sill

Note: Data presented and discussed by Link et al. (1993). *N*—Number of localities, *D* and *I*—declination and inclination after bedding correction, *k*—Fisher precision, α_{95}—95% confidence interval about mean direction, A_{95}—95% confidence interval about pole, N/R—polarity.

be presumed to be the product of plate interactions. Because of the stratigraphic control, the early part of the Grand Canyon polar path still can be considered valid and adequate to reflect cratonic movement. We also have the ascending leg of the Elsonian apparent polar wander path go through the well-established 1250 Ma poles for the MacKenzie and Sudbury dikes (C-5 and C-6, Fig. 8). Beginning with the pole for strata at the base of the Shinumo Quartzite and a long episode of essentially continuous deposition, the Unkar-Nankoweap poles trace out an APW loop that is independently observed and closely correlated with poles from the Keweenawan rift system (Fig. 8). The close correspondence of these paths confirms the existence of the ''Unkar-Keweenawan loop'' and serves to refine the true nature of the Keweenawan loop (Link et al., 1993). Furthermore, we observe no significant vertical-axis rotation of the Colorado Plateau (which would be marked by an offset between the two polar paths).

Vertical-Axis Rotations and Deformation

To a first order, paleomagnetic data indicate that the Belt-Purcell basin has remained a simple rigid body since deposition. Norris and Black's early study (1961) was designed to test the hypothesis (Price, 1958) that a curved orogenic front, the ''Crowsnest deflection,'' formed by the Lewis fault and associated fold-and-thrust structures in southern Alberta, was an orocline. They did not find magnetizations with directions fanned around this structure as predicted by the orocline hypothesis. Our data confirm a lack of fanning in magnetization directions and thus the ''Crowsnest deflection'' can be ascribed to the superposition of younger east-directed motion on thrusts and folds upon older northeast-directed thrusts and folds (Price, 1967).

Our paleomagnetic data set additionally reveals second-order deformation within the basin. The locality means plotted in Figure 3 tend to have elongated distributions along lines of constant inclination. This pattern is the signature of relative vertical-axis rotations that typically occur in fault-divided regions. Only two localities in our entire study show evidence of large (>30°) rotations relative to the basin as a whole: (1) Purcell Lava flows sampled at Bull River (PLbur) within the Rocky Mountain Trench and (2) Bonner Quartzite sampled at Schwartz Creek (Bsc) on the south side of the Lewis and Clark structural discontinuity exhibit strongly CW-rotated directions (Fig. 3). These directions were probably rotated by a component of dextral strike-slip displacement along their associated faults.

Price and Sears (2001) reported <20 km of shortening between cratonic North America and the Belt-Purcell basin along latitude line 47°N; farther north, at 49° or 50°N, they recognized ~250 km of Cretaceous shortening. From this, they hypothesized that the entire basin underwent a CW rotation of 30° relative to the North American craton about an Euler pole near Helena, Montana (lat 110°W, long 46.5°N). However, on comparing Belt-Purcell poles to the Electra Lake Gabbro and Sibley Group poles (Fig. 8), we infer an insignificant rigid-body clockwise rotation of 4° ± 5°. In the extreme case, comparing the Electra Lake Gabbro pole to the upper member of the Mount Shields Formation pole, we find a CW rotation of 19° ± 4°, far short of 30°. Therefore, much of the apparent rotation predicted by Price and Sears must have been accommodated along complementary faults within the basin.

Comparison of Geologically and Geophysically Determined Rates and Processes

The great thickness of the Belt-Purcell Supergroup led several workers to propose that the section accumulated over several hundred million years (e.g., Harrison and Peterman, 1984). However, the paleomagnetic record

from the Belt-Purcell basin has always indicated that its deposition occurred in a considerably shorter interval of time (e.g., Evans et al., 1975; Elston, 1984; Link et al., 1993). The publication of U-Pb ages for the top of the Belt-Purcell Supergroup (Evans et al., 2000) firmly establishes that total duration was between 50 and 100 m.y.

A remarkable aspect of the Belt-Purcell paleomagnetic record is the existence of (1) a few long stratigraphic intervals of single polarity recorded in sediment accumulations of several kilometers and (2) a stratigraphically appreciable interval of mixed polarity with meter-scale reversals (Fig. 5). This mixed-polarity interval, corresponding with the accumulation of the upper member of the Mount Shields Formation, was a time of pronounced, apparently rapid APW, accompanied by an increase in deposition of coarse clastic sediment. This movement was followed by an abrupt halt and change in direction of APW, in turn corresponding with deposition of the coarse-grained Bonner Quartzite. Except for the sub-Shepard unconformity (falling within the middle reversed-polarity zone), no significant unconformities have been observed or reported by workers in the Belt-Purcell succession (e.g., Link, 1998). The sub-Shepard unconformity is a sharp unweathered break in sedimentation and at a few places displays ~0.3 m of abrupt relief, possibly of wave-cut origin; erosional debris on the disconformity appears to be lacking. In Canada, however, this horizon is marked by a prominent unconformity and an associated conglomerate layer (Höy, 1993). Otherwise unconformities that would significantly reduce the number of observable polarity chrons are lacking.

In Figure 4, the polarity record of the Belt-Purcell Supergroup (plotted by arbitrarily giving each formation equal duration) is compared to the geomagnetic polarity time scale for the past 160 m.y. The number of reversals observed in the Belt-Purcell paleomagnetic record is far lower than during any 50–100 m.y. window in the Late Cretaceous and Cenozoic record. However, if the middle reversed zone in the Belt-Purcell section happens to have recorded a long superchron, such as the middle Cretaceous long normal superchron, reversal rates then were comparable.

In Figure 9, we plot the paleolatitude evolution of a reference point (lat 48°N, long 115°W) during deposition by using the Belt-Purcell APWP, and as a first approximation, we assume that each formation marks an equal increment of time. The evolution curves are stretched over intervals of 50–400 m.y. duration. We compare these curves to the paleo-

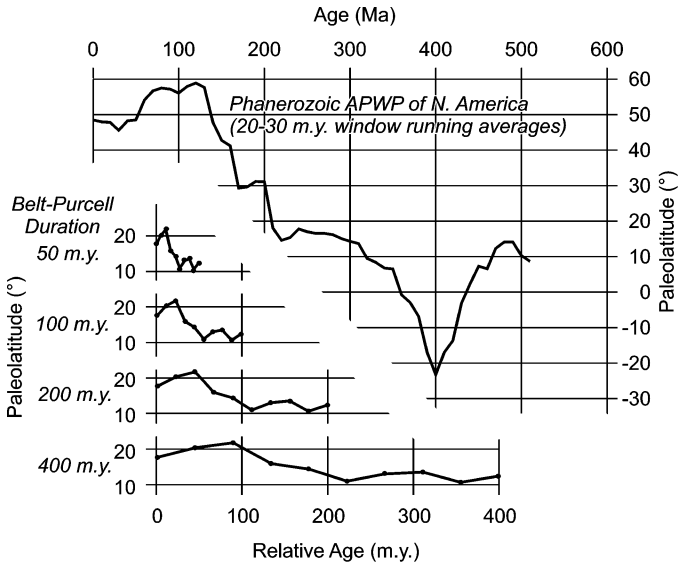

Figure 9. Comparison of Belt-Purcell to Phanerozoic paleolatitude evolution. The reference point lies within the Belt-Purcell basin (48°N, 115°W). The Belt-Purcell points are equally spaced to allow for first-order comparison. Similarities between the Phanerozoic and Belt-Purcell curves are seen for the 50 and 100 m.y. durations, showing approximately constant and equivalent plate-tectonic rates.

latitude evolution for the same point determined from the Phanerozoic APWP of North America (Besse and Courtillot, 1991; Van der Voo, 1990; Wynne et al., 1992). A statistically rigorous comparison is not possible because the Phanerozoic APWP was produced by calculating 20–30 m.y. window averages and the Belt-Purcell APWP by calculating formation averages.

The reference point remained at ~12°N from the time of deposition of the Spokane Formation to deposition of the middle member of the Mount Shields Formation and then abruptly shifted to ~20°N from the time of deposition of the upper member of the Mount Shields Formation to deposition of the Pilcher Quartzite. This modest paleolatitude variation is similar in magnitude to the paleolatitude variation over the past 100 m.y. (or the 50 m.y. from 75 Ma to 25 Ma) and is very much less than that observed over any Phanerozoic window of 200 or 400 m.y. This first-order comparison suggests that a duration of 50–100 m.y. for deposition of the Belt-Purcell Supergroup is fully compatible with Phanerozoic rates of APW. We conclude that Middle Proterozoic rates of plate motion did not differ significantly from Phanerozoic rates. This conclusion is reinforced by considering the paleolatitude evolution of the Grand Canyon, by using the data of Table 4. The observed variation of ~60° latitude, occurring twice over ~400 m.y., is much like similar periods of plate motion derived from the Phanerozoic polar path.

One major observation derived from the entire Middle Proterozoic APWP is that the Belt-Purcell Supergroup was deposited during an important hairpin turn, similar to the hairpin turns recorded during Unkar-Keweenawan (Grenville) time (Fig. 8). A similar hairpin turn is recognized for the Cretaceous (e.g., Besse and Courtillot, 1991). For the Belt-Purcell Supergroup, the long interval of reverse polarity can be estimated to be ~40 m.y. in length (Fig. 4). Long intervals of normal polarity characterize the ascending and descending legs of the Unkar loop, each ~50 m.y. in length (Fig. 8). These three stable polarity intervals are comparable in length to the 40 m.y. Cretaceous long normal-polarity interval (Harland et al., 1990).

Hairpin turns in an APWP mark major tectonic reorganizations (e.g., Irving and Park, 1972). We note that APWP cusps at the times of deposition of G4 (Shinumo Quartzite) and G7–G8 (upper middle Dox Sandstone) (Fig. 8) both correspond to times of numerous asymmetrical reversals that are stratigraphically very closely spaced and are restricted to individual beds and even parts of beds. It also should be noted that these abundant asymmetric reverse-polarity remanences lie between strata holding normal-polarity remanences whose pole positions (G7 and G8) control the ca. 1100 Ma apex of the Unkar-

Keweenawan loop. The correspondence of episodes of tectonism with (1) times when plate movements come to a halt and then change direction; and (2) when polarity reversals become abundant suggests the existence of a genetic interrelationship between (a) crustal reorganization, (b) inferred disruption and restoration of core and mantle flow regimes, and (c) presumed variations in heat transfer through impeded and unimpeded mantle convection.

We propose that several ~50 m.y. periods of Earth history have been characterized by stable paleomagnetic fields and that the stable fields corresponded with times of relative tectonic stability. Such paleomagnetically stable intervals include (1) the long Cretaceous normal superchron, (2) the reverse-polarity Pennsylvanian–Permian superchron, (3) the normal-polarity intervals preceding and following the climax of late Middle Proterozoic Keweenawan (Grenville) orogenesis, and (4) the middle Elsonian reverse-polarity interval recorded in the Belt-Purcell Supergroup. The middle Cretaceous superplume proposed by Larson (1991) developed between Jurassic tectonism and the onset of the Late Cretaceous Laramide orogeny. Stability of the paleomagnetic field seems to correlate with times when heat-flow and heat-loss regimes, from core to crust, were unimpeded by plate-tectonic interactions and collisions and mantle plumes and superplumes may have been able to develop fully and transport heat from core to mantle (Larson and Olson, 1991).

CONCLUSIONS

The Belt-Purcell Supergroup has provided excellent paleomagnetic results from which we have obtained definitive insight into the formation and deformation of a large region of the western North American craton. We report results from >2700 samples from 93 localities, spanning 13 formations and members of formations. All the shallow-marine formations overlying the Lower Belt Group turbidites contain red sediments or hematite-bearing lavas with highly stable remanence properties. Paleomagnetic directions pass the tilt test, indicating that they predate Cretaceous tilting. Even more significantly, the strata display a magnetostratigraphically coherent directional and polarity evolution, demonstrating that an original magnetization has been retained across a large part of the succession.

Paleomagnetic directions do not change greatly from formation to formation, and few polarity switches were found across much of the Belt-Purcell succession. For two decades, the paleomagnetic record has been used to argue for a relatively short duration of deposition. Geochronological studies now restrict the duration of Belt-Purcell deposition to <100 m.y. There are important geodynamic implications to the new understanding of the Belt-Purcell basin development rate described here, but major unanswered questions remain. For example, how is it that a 20 km sink developed adjacent to an otherwise stable craton and then remained little disturbed for the following 1.4 b.y.?

We herein resolve the controversy concerning Belt-Purcell poles and apparently incompatible poles from Elsonian anorogenic intrusions of Labrador and contemporary poles from the Laurentian Shield. These poles, here informally assigned to three periods, do not conflict but rather trace out a south-trending hairpin loop. The Belt-Purcell poles plot at the southern end of the loop and fill in a gap between poles from early and late Elsonian igneous rocks. A younger north- and then south-trending loop, similar in amplitude and duration to the Elsonian path, is recognized for the Middle Proterozoic Unkar and Keweenawan Supergroups. A polar wander loop also exists for the Cretaceous of North America. Similar patterns of polar wander recorded during Middle Proterozoic to Phanerozoic time appear to reflect continental drift and times and places marking plate interactions and episodes of tectonism and orogenesis.

ACKNOWLEDGMENTS

Elston

The USGS study in the Belt basin of Montana and Idaho owes its success to the geologic support of many colleagues and the support of project work by the Geologic Framework and Synthesis Program. The U.S. National Park Service is thanked for permission to sample in Glacier National Park and for permission to contract for helicopter transport into several particularly remote localities. Other sampling localities were mostly in exposures along highways and many logging roads. I particularly acknowledge and thank several geologists who directed us to outcrops favorable for paleomagnetic study; they willingly shared hard-won information concerning details of the stratigraphy, structure, and facies changes gleaned from geologic mapping in the region. J.E. Harrison (deceased) deserves special mention. He guided us to many sampling sites and arranged for us to work with several other geologists who were mapping in the region. Other geologists whose help is also gratefully acknowledged include, in approximate order of interaction—Melvin R. Mudge, Robert G. Schmidt (deceased), Robert Earhart, Chester A. Wallace, Edward T. Ruppel, Warren B. Hobbs, E-an Zen, and Mitchell R. Reynolds. E.T. Ruppel provided a memorable pack trip to the crest of the Lemhi Range where the lower Swauger Quartzite was sampled. I wish to acknowledge the participation of S.L. Bressler, who on several occasions led one of two sampling teams that were simultaneously placed in the field and staffed by student geologists. Many of these students also were involved with the laboratory analysis of considerable parts of a very large data set. In particular, the participation and aid in the field and laboratory of several students is acknowledged with thanks and appreciation. A partial list includes Michael Ahkeah, Roy Ayala, Denise Byers, Gary Calderone, Karen Chase, Nancy Johnson, Albert Luna, Gary Mercado, and Deborah Rineer. The omission of any individual has been inadvertent. Shirley Elston routinely participated in the collection of samples. Lastly, I thank C.A. Wallace for his extensive review of a previous manuscript dealing with the USGS work. E.T. Ruppel and P.K. Link are also thanked for their reviews and comments, and J.E. Harrison and J. Connor for their comments on the previous manuscript. That manuscript served as the point of departure that led to this analysis, to a refined interpretation of the Belt paleomagnetic data set, and to this paper.

Enkin, Baker, and Kisilevsky

We thank Kirk Osadetz for introducing us to this study and guiding the field work. Cameron Watson assisted in the field, Paula Wheadon assisted in the lab, and Richard Franklin assisted with drafting. We thank Ray Price, Derek Brown, and Paul Link for sharing their knowledge of the Belt-Purcell basin. Ted Irving, Jim Sears, Doug Elmore, and Gerry Ross provided detailed and helpful reviews.

REFERENCES CITED

Aleinikoff, J.N., Evans, K.V., Fanning, C.M., Obradovich, J.D., Ruppel, E.T., Zieg, J.A., and Steinmetz, J.C., 1996, SHRIMP U-Pb ages of felsic igneous rocks, Belt Supergroup, western Montana: Geological Society of America Abstracts with Programs, v. 28, no. 7, p. 376.

Anderson, H.E., and Davis, D.W., 1995, U-Pb geochronology of the Moyie Sills, Purcell Supergroup, southeastern British Columbia: Implications for the Mesoproterozoic geological history of the Purcell (Belt) basin: Canadian Journal of Earth Sciences, v. 32, p. 1180–1193.

Barton, J.M., Jr., 1974, Progress of isotopic and geochemical investigations, coastal Labrador, 1973: Geology Department, University of Massachusetts, no. 13, The Nain Anorthosite Project, Labrador; Field Report 1973, p. 19–28.

Besse, J., and Courtillot, V., 1991, Revised and synthetic apparent polar wander paths of the African, Eurasian, North American and Indian plates, and true polar wander since 100 Ma: Journal of Geophysical Research, v. 96, p. 4029–4050.

Black, R.F., 1963, Palaeomagnetism of part of the Purcell System in southwestern Alberta and southeastern British Columbia: Geological Survey of Canada Bulletin 83, p. 1–31.

Bressler, S.L., and Elston, D.P., 1980, Declination and inclination errors in experimentally deposited specularite-bearing sand: Earth and Planetary Science Letters, v. 48, p. 227–232.

Brown, D.A., and Woodfill, R.D., 1998, The Moyie Industrial Partnership Project; geology and mineralization of the Yahk-Moyie Lake area, southeastern British Columbia (82F/01E, 82G/04W, 82F/08E, 82G/05W): Victoria, British Columbia Geological Division, Geological Fieldwork 1998, p. 9.1–9.22.

Buchan, K.L., Mertanen, S., Park, R.G., Pesonen, L.J., Elming, S.-Å., Abrahamsen, N., and Bylund, G., 2000, Comparing the drift of Laurentia and Baltica in the Proterozoic: The importance of key palaeomagnetic poles: Tectonophysics, v. 319, p. 167–198.

Collinson, D.W., and Runcorn, S.K., 1960, Polar wandering

and continental drift: Evidence of paleomagnetic observations in the United States: Geological Society of America Bulletin, v. 71, p. 915–958.

Doughty, P.T., and Chamberlain, K.R., 1996, Salmon River arch revisited: New evidence for 1370 Ma rifting near the end of deposition in the Middle Proterozoic Belt basin, Canadian Journal of Earth Sciences, v. 33, p. 1037–1052.

Doughty, P.T., Price, R.A., and Parish, R.R., 1998, Geology and U-Pb geochronology of Archean basement and Proterozoic cover in the Priest River complex, northwestern United States, and their implications for the Cordilleran structure and Precambrian continent reconstructions: Canadian Journal of Earth Sciences, v. 35, p. 39–54.

Elston, D.P., 1984, Magnetostratigraphy of the Belt Supergroup, A synopsis, *in* Hobbs, S.W., ed., The Belt; Abstracts and summaries, Belt symposium II, 1983: Montana Bureau of Mines and Geology Special Publication 90, p. 88–90.

Elston, D.P., 1989, Grand Canyon Supergroup, northern Arizona; Stratigraphic summary and preliminary paleomagnetic correlations with parts of other North American Proterozoic successions, *in* Jenney, J.P., and Reynolds, S.J., eds., Geologic evolution of Arizona: Arizona Geological Society Digest 17, p. 259–272.

Elston, D.P., 1991, Geologic and paleomagnetic evidence for an ~1300 Ma tectonic event in the Missoula Group, Belt Supergroup (~1450–1250 Ma), Montana and Idaho: Geological Society of America Abstracts with Programs, v. 23, no. 4, p. 423–433.

Elston, D.P., and Bressler S.L., 1980, Paleomagnetic poles and polarity zonation from the Middle Proterozoic Belt Supergroup, Montana and Idaho: Journal of Geophysical Research, v. 85, p. 339–355.

Elston, D.P., and Grommé, C.S., 1974, Precambrian polar wandering from Unkar Group and Nankoweap Formation, eastern Grand Canyon, Arizona, *in* Karlstrom, T.N.V., Swann, G.A., and Eastwood, R.L., eds., Geology of northern Arizona with notes on archaeology and paleoclimate; Pt. 1, Regional studies: Flagstaff, Northern Arizona University, Geological Society of America Rocky Mountain Section Meeting, p. 97–117.

Elston, D.P., and McKee, E.H., 1982, Age and correlation of the Late Proterozoic Grand Canyon disturbance, northern Arizona: Geological Society American Bulletin, v. 93, p. 681–699.

Elston, D.P., and Purucker, M.E., 1979, Detrital magnetization in red beds of the Moenkopi Formation (Triassic), Gray Mountain, Arizona: Journal of Geophysical Research v. 84B, p. 1653–1665.

Elston, D.P., and Scott, G.R., 1973, Paleomagnetism of some Precambrian flows and red beds, eastern Grand Canyon, Arizona: Earth and Planetary Science Letters, v. 18, p. 253–265.

Enkin, R.J., Osadetz, K.G., Baker, J., and Kisilevsky, D., 2000, Orogenic remagnetizations in the front ranges and inner foothills of the southern Canadian Cordillera: Chemical harbinger and thermal handmaiden of Cordilleran deformation: Geological Society of America Bulletin, v. 112, p. 929–942.

Evans, K.V., and Fisher, L.B., 1986, U-Pb geochronology of two augen gneiss terranes, Idaho: New data and tectonic implications: Canadian Journal of Earth Sciences, v. 23, p. 1919–1927.

Evans, M.E., Bingham, D.K., and McMurry, E.W., 1975, New paleomagnetic results from the upper Belt-Purcell Supergroup of Alberta: Canadian Journal of Earth Sciences, v. 12, p. 52–61.

Evans, K.V., Aleinikoff, J.N., Obradovich, J.D., and Fanning, C.M., 2000, SHRIMP U-Pb geochronology of volcanic rocks, Belt Supergroup, western Montana: Evidence for rapid deposition of sedimentary strata: Canadian Journal of Earth Sciences, v. 37, p. 1287–1300.

Franklin, J.M., 1978, The Sibley Group, Ontario, *in* Wanless, R.K., and Loveridge, W.D., eds., Rubidium-strontium isotopic age studies, Report 2 (Canadian Shield): Geological Survey of Canada Paper 77–14, p. 31–34.

Halls, H.C., and Pesonen, L.J., 1982, Paleomagnetism of Keweenawan rocks, *in* Wold, R.J., and Hinze, W.J., eds., Geology and tectonics of the Lake Superior basin: Geological Society of America Memoir 156, p. 173–201.

Hamilton, M.A., Emslie, R.F., and Roddick, J.C., 1994, Detailed emplacement chronology of basic magmas of the mid-Proterozoic Nain plutonic suite, Labrador; insights from U-Pb systematics in zircon and baddeleyite: Reston, Virginia, U.S. Geological Survey, Abstracts of the Eighth International Conference on Geochronology, Cosmochronology and Isotope Geology, p. 124.

Harlan, S.S., and Geissman, J.W., 1998, Paleomagnetism of the Middle Proterozoic Electra Lake Gabbro, Needle Mountains, southwestern Colorado: Journal of Geophysical Research, v. 103, p. 15497–15507.

Harlan, S.S., Snee, L.W., Geissman, J.W., and Brearley, A.J., 1994, Paleomagnetism of the Middle Proterozoic Laramie anorthosite complex and Sherman Granite, southern Laramie Range, Wyoming and Colorado: Journal of Geophysical Research, v. 99, p. 17997–18020.

Harland, W.B., Armstrong, R.L., Cox, A.V., Craig, L.E., Smith, A.G., and Smith, D.G., 1990, A geological time scale 1989: Cambridge, UK, Cambridge University Press, 263 p.

Harrison, J.E., 1972, Precambrian Belt basin of northwestern United States: Its geometry, sedimentation, and copper occurrences. Geological Society of America Bulletin, v. 83, p. 1215–1240.

Harrison, J.E., and Peterman, Z.E., 1984, Introduction to correlation of Precambrian rock sequences: U.S. Geological Survey Professional Paper 1241-A, 7 p.

Harrison, J.E., Griggs, A. B., and Wells, J.D., 1986, Geologic and structure maps of the Wallace 1° × 2° Quadrangle, Montana and Idaho: U.S. Geological Survey Miscellaneous Investigations Map I-1509-A, scale 1: 250 000.

Hoffman, P.F., 1989, Precambrian geology and tectonic history of North America, *in* Bally, A.W., and Palmer, A.W., eds., The geology of North America: An Overview: Boulder, Colorado, Geological Society of America, Geology of North America, v. A, p. 447–512.

Höy, T., 1989, The age, chemistry, and tectonic setting of the Middle Proterozoic Moyie sills, Purcell Supergroup, southeastern British Columbia: Canadian Journal of Earth Sciences, v. 26, p. 2305–2317.

Höy, T., 1993, Geology of the Purcell Supergroup in the Fernie west-half map area, southeastern British Columbia: British Columbia Ministry of Energy, Mines and Petroleum Resources, Geological Survey Branch, Bulletin 84, 157 p.

Irving, E., and Park, J.K., 1972, Hairpins and superintervals: Canadian Journal of Earth Sciences, v. 9, p. 1318–1324.

Irving, E. and Wynne, P.J., 1991, Paleomagnetism: Review and tectonic implications, Chapter 3, *in* Gabrielse, H., and Yorath, C.J., eds., Geology of the Cordilleran orogen in Canada: Geological Survey of Canada Geology of Canada, no. 4, and Geological Society of America, Geology of North America, v. G-2, p. 61–86.

Kidder, D.L., 1988, Syntectonic sedimentation in the Proterozoic upper Belt Supergroup, northwestern Montana: Geology, v. 16, p. 658–661.

Kirschvink, J.L., 1980, The least-squares line and plane and the analysis of paleomagnetic data: Geophysical Journal of the Royal Astronomical Society, v. 62, p. 699–718.

Kisilevsky, D.K., 1998, A palaeomagnetic study of the Lewis thrust sheet, southeast Canadian Rocky Mountains: Structural and tectonic implications [M.Sc. thesis]: Kingston, Ontario, Queen's University, 97 p.

Larson, R.L., 1991, Latest pulse of the Earth: Evidence for a mid-Cretaceous superplume: Geology, v. 19, p. 547–550.

Larson, R.L., and Olson, P., 1991, Mantle plumes control magnetic reversal frequency: Earth and Planetary Science Letters, v. 107, p. 437–447.

Lewchuk, M.T., Al-Aasm, I.S., Symons, D.T.A., and Gillen, K.P., 1996, Paleomagnetism, petrography and isotope geochemistry of unoriented drill core from the Mississippian Mount Head Formation of the Shell Waterton gas field in southwest Alberta, Canada [abs.]: Eos (Transactions, American Geophysical Union), v. 77, no. 46, p. 159.

Link, P.K., Christie-Blick, N., Devlin, W.J., Elston, D.P., Horodyski, R.J., Levy, M., Miller, J.M.G., Pearson, R.C., Prave, A., Stewart, J.H., Winston, D., Wright, L.A., and Wruke, C.T., 1993, Middle and Late Proterozoic stratified rocks of the western U.S., Cordillera, Colorado Plateau, and Basin and Range province, *in* Reed, J.C., Jr., Bickford, M.E., Houston, R.S., Link, P.K., Rankin, D.W., Sims, P.K., and Van Schmus, W.R., eds., Precambrian: Conterminous U.S.: Boulder, Colorado, Geological Society of America, Geology of North America, v. C-2, p. 463–595.

Link, P.K., 1998, Regional geologic perspectives on the Belt Supergroup gained since the Belt Symposium II, 1983, *in* Berg, Richard B., ed., Proceedings of the Belt Symposium III: Montana Bureau of Mines and Geology Special Publication 112, p. 2–10.

Maxwell, D.T., and Hower, J., 1967, High-grade diagenesis and low-grade metamorphism of illite in the Precambrian Belt Series: American Mineralogist, v. 52, p. 843–857.

McMechan, M.E., 1981, The Middle Proterozoic Purcell Supergroup in the southeastern Rocky and southeastern Purcell Mountains, British Columbia and the initiation of the Cordilleran miogeocline, southern Canada and adjacent United States: Bulletin of Canadian Petroleum Geology v. 29, p. 583–621.

McMechan, M.E., and Price, R.A., 1982, Transverse folding and superposed deformation, Mount Fisher area, southern Canadian Rocky Mountain thrust and fold belt: Canadian Journal of Earth Sciences, v. 19, p. 1011–1024.

Morris, W.A., and McMechan, M.E., 1983, Paleomagnetism of the Middle Proterozoic Mount Nelson Formation: Evidence for a regional remagnetization event in the late Precambrian of the Cordillera: Canadian Journal of Earth Sciences, v. 20, p. 561–567.

Murthy, G.S., 1978, Paleomagnetic results from the Nain anorthosite and their tectonic implications: Canadian Journal of Earth Sciences, v. 15, p. 516–525.

Norris, D.K., and Black, R.F., 1961, Application of palaeomagnetism to thrust mechanics: Nature, v. 192, p. 933–935.

Obradovich, J.D., and Peterman, Z.E., 1968, Geochronology of the Belt Series, Montana: Canadian Journal of Earth Sciences, v. 5, p. 737–747.

Osadetz, K.G., Kohn, B., Feinstein, S., and Price, R.A., 1995, Lewis plate thermal and geological history from fission-track data [abs.]: Victoria, British Columbia, Geological Association of Canada/Mineralogical Association of Canada, Joint Annual Meeting, p. A-78.

Palmer, H.C., and Halls, H.C., 1986, Paleomagnetism of the Powder Mill Group, Michigan and Wisconsin: A reassessment of the Logan Loop: Journal of Geophysical Research, v. 91, no. 11, p. 11571–11580.

Park, J.K., and Roy, J.L., 1979, Further paleomagnetic results from the Seal Group igneous rocks, Labrador: Canadian Journal of Earth Sciences, v. 16, p. 895–912.

Price, R.A., 1958, Structure and stratigraphy of the Flathead north map-area (east-half), British Columbia and Alberta [Ph.D. thesis]: Princeton, New Jersey, Princeton University, 363 p.

Price, R.A., 1965, Flathead map-area, British Columbia and Alberta: Geological Survey of Canada Memoir 336, 221 p.

Price, R.A., 1967, The tectonic significance of mesoscopic subfabrics in the southern Rocky Mountains of Alberta and British Columbia: Canadian Journal of Earth Sciences, v. 4, p. 39–70.

Price, R.A., and Sears, J.W., 2001, A preliminary palinspastic map of the Mesoproterozoic Belt-Purcell Supergroup, Canada and USA.: Implications for the tectonic setting and structural evolution of the Purcell anticlinorium and the Sullivan deposit, *in* Lydon, J.W., Slack, J.F., Höy, T., and Knapp, M.E., eds., The geological environment of the Sullivan deposit, British Columbia: Geological Association of Canada, Mineral Deposits Division, MDD Special Volume 1, p. 44–63.

Purucker, M.E., Elston, D.P., and Shoemaker, E.M., 1980, Early acquisition of stable magnetization in red beds

of Triassic Moenkopi Formation, Gray Mountain, Arizona: Journal of Geophysical Research, v. 85B, p. 997–1012.

Robertson, W.A., 1973, Pole position from thermally cleaned Sibley Group sediments and its relevance to Proterozoic magnetic stratigraphy: Canadian Journal of Earth Sciences, v. 10, p. 180–193.

Romer, R.L., Schaerer, U., Wardle, R.J., and Wilton, D.H.C., 1995, U-Pb age of the Seal Lake Group, Labrador; relationship to Mesoproterozoic extension-related magmatism of Laurasia: Canadian Journal of Earth Sciences, v. 32, p. 1401–1410.

Ross, G.M., Parrish, R.R., Villeneuve, M.E., and Bowring, S.A., 1991, Geophysics and geochronology of the crystalline basement of the Alberta basin, western Canada: Canadian Journal of Earth Sciences, v. 28, p. 512–522.

Ross, G.M., Parrish, R.R., and Winston, D., 1992, Provenance and U-Pb geochronology of the Mesoproterozoic Belt Supergroup (northwestern United States): Implications for age of deposition and pre-Panthalassa plate reconstructions: Earth and Planetary Science Letters, v. 113, p. 57–76.

Roy, R.L., and Fahrig, W.F., 1973, The paleomagnetism of the Seal and Croteau rocks from the Grenville front, Labrador: Polar wandering and tectonic implications: Canadian Journal of Earth Sciences, v. 10, p. 1279–1301.

Runcorn, S.K., 1964, Paleomagnetic results from Precambrian sedimentary rocks in the western United States: Geological Society of America Bulletin, v. 75, p. 687–704.

Schandl, E.S., and Davis, D.W., 2001, Geochronology of the Sullivan deposit: U-Pb and Pb-Pb ages of zircon and titanites, *in* Lydon, J.W., Slack, J.F., Höy, T., and Knapp, M.E., eds., The geological environment of the Sullivan deposit, British Columbia: Geological Association of Canada, Mineral Deposits Division, MDD Special Volume 1, p. 111–120.

Sears, J.W., Chamberlain, K.R., and Buckley, S.N., 1998, Structural and U-Pb geochronological evidence for 1.47 Ga rifting in the Belt basin, western Montana: Canadian Journal of Earth Sciences, v. 35, p. 467–475.

Stuckey, W., Meert, J.G., Pullen, C.E., and Wells, T., 1999, Paleomagnetic investigations of the St. Francois igneous province, Missouri: Testing mid-Proterozoic paleopoles from Laurentia: Eos (Transactions, American Geophysical Union), v. 80, suppl., p. F299.

Symons, D.T.A., and Timmons, E.A., 1992, Geotectonics of the cratonic margin from paleomagnetism of the Middle Proterozoic Aldridge (Prichard) Formation and Moyie sills of British Columbia and Montana: Basement Tectonics, v. 8, p. 373–384.

Timmons, J.M., Karlstrom, K.E., Dehler, C.M., Geissman, J.W., and Heizler, M.T., 2001, Proterozoic multistage (ca. 1.1 and 0.8 Ga) extension recorded in the Grand Canyon Supergroup and establishment of northwest- and north-trending tectonic grains in the southwestern United States: Geological Society of America Bulletin, v. 113, p. 163–180.

Van der Voo, R., 1990, Paleozoic paleomagnetic poles from Europe and North America and comparisons with continental reconstructions: Reviews of Geophysics, v. 28, p. 167–206.

Vitorello, I., and Van der Voo, R., 1977, Late Hadrynian and Helikian pole positions from the Spokane Formation, Montana: Canadian Journal of Earth Sciences, v. 14, p. 67–73.

Walcott, C.D., 1899, Pre-Cambrian fossiliferous formations: Geological Society of America Bulletin, v. 10, p. 199–244.

Wanless, R.K., and Loveridge, W.D., 1978, Rubidium-strontium isotopic age studies, report 2 (Canadian Shield): Geological Survey of Canada Paper 77-14, 70 p.

Watson, G.S., and Enkin, R.J.E., 1993, The fold test in paleomagnetism as a parameter estimation problem: Geophysical Research Letters, v. 20, p. 2135–2137.

Weil, A.B., Van der Voo, R., Mac Niocail, C., and Meert, J.G., 1998, The Proterozoic supercontinent Rodinia; paleomagnetically derived reconstructions for 1100–800 Ma: Earth and Planetary Science Letters, v. 154, p. 13–24.

Wells, J.B., 1974, Geologic map of the Alberton Quadrangle, Missoula, Saunders, and Mineral Counties, Montana: U.S. Geological Survey Geologic Quadrangle Map GQ-1157, scale 1:62 500.

Whipple, J.W., and Johnson, S.N., 1988, Stratigraphy and lithocorrelation of the Snowslip Formation (Middle Proterozoic Belt Supergroup), Glacier National Park, Montana: U.S. Geological Survey Bulletin 1833, 30 p.

Winston, D., 1986, Stratigraphic correlation and nomenclature of the Middle Proterozoic Belt Supergroup: A guide to Proterozoic rocks of western Montana and adjacent areas: Montana Bureau of Mines and Geology Special Publication 94, p. 69–84.

Winston, D., 1989, A sedimentologic and tectonic interpretation of the Belt, *in* Winston, D., Horodyski, R.J., and Whipple, J.W., eds., Middle Proterozoic Belt Supergroup, western Montana: American Geophysical Union, 28th International Geological Congress Field Trip Guidebook T334, p. 47–69.

Wynne, P.J., Irving, E., Schulze, D.E., Halls, D.C., and Helmstaedt, H.H., 1992, Paleomagnetism of three Canadian Rocky Mountain diatremes: Canadian Journal of Earth Sciences, v. 29, p. 35–47.

Yu, Y., and Morse, S.A., 1993, $^{40}Ar/^{39}Ar$ chronology of the Nain anorthosites, Canada: Canadian Journal of Earth Sciences, v. 30, p. 1166–1178.

Zartman, R.E., Peterman, Z.E., Obradovich, J.D., Gallego, M.D., and Bishop, D.T., 1982, Age of the Crossport C sill near Eastport, Idaho, *in* Reid, R.R., and Williams, G.A., Society of Economic Geologists, Coeur d'Alene Field Conference: Idaho Bureau of Mines and Geology Bulletin 24, p. 61–69.

MANUSCRIPT RECEIVED BY THE SOCIETY DECEMBER 5, 2000
REVISED MANUSCRIPT RECEIVED OCTOBER 25, 2001
MANUSCRIPT ACCEPTED NOVEMBER 19, 2001

Printed in the USA